Andrea Cipollini and Fabio Parla*

Temperature and Growth: Seasonal and Non-Linear Effects Using EU Subnational Data

https://doi.org/10.1515/snde-2025-0108
Received August 1, 2025; accepted January 28, 2026; published online February 19, 2026

Abstract: We study the impact of temperature on aggregate and sector-specific growth in gross value added using regional EU data observed over 1980 – 2019 using a mixed frequency dataset. The regional data on economic growth are annual and, since there is wide consensus on projections of a temperature rise more concentrated during fall-winter than spring-summer, we focus on seasonal region-specific temperature shocks and on their interaction also with global seasonal temperature of a given year. The empirical analysis, based on panel local projections, suggests no evidence of adaptation and projections of large losses during hot seasons under a scenario of no implementation of climate change mitigation policies. Investments are important transmission channels driving a negative effect on growth due to a one-degree Celsius increase in the level of seasonal temperature. Moreover, construction is the most vulnerable sector, and the regions with a higher income per capita or competitiveness are the most resilient to temperature shocks.

Keywords: temperature shocks; seasonality; EU regional economic growth; local projection

JEL Classification: C33; Q54; R11

1 Introduction

The focus of this study is the analysis of the impact of rising seasonal temperatures on economic growth using sub-national data for Europe. The recent Annual Climate Highlights report by Copernicus (see Copernicus Climate Change Service/ECMWF 2022) shows, for Europe, the hottest summer ever recorded, and the highest rate of increase of any continent in the world (European temperatures have increased by more than twice the global average over the past 30 years). Consequently, it has become more stringent a prompt action by

Andrea Cipollini and Fabio Parla contributed equally to this work. The data supporting the findings of this study are available within the Supplementary Materials.
We would like to thank the editor Jeremy Piger and the associate editor, as well as participants at the 9th International Conference on Applied Theory, Macro and Empirical Finance (AMEF 2025), the Second International Conference on the Climate-Macro-Finance Interface, the 1st CAM-Risk conference, the EMCC VIII conference, the RCEA 2024, the MSBE Group Research Seminar 2024 (University of Edinburgh Business School), the IWEEE2024, the CEF 2023, the IAAE 2023 Annual Conference, the ICEEE 2023, and the CFE-CMStatistics 2022 for their useful comments and suggestions. We would like to thank also the European Centre for Medium-Range Weather Forecasts (ECMWF) for sharing detailed information about data aggregation at the NUTS2 level used in the Copernicus Climate Data Store (CDS). The results of this work are based on Copernicus Climate Change Service information. Neither the European Commission nor ECMWF is responsible for any use that may be made of the Copernicus information or data it contains. Source for statistical units: Eurostat, © EuroGeographics for the administrative boundaries. This research work has been carried out with the co-financing of the European Union – FESR o FSE, PON Ricerca e Innovazione 2014–2020 – DM 1062/2021. Declarations of interest: none. The usual disclaimer applies.

***Corresponding author: Fabio Parla**, Department of Economics, Business and Statistics, University of Palermo, Viale delle Scienze, 90128 Palermo, Italy, E-mail: fabio.parla@unipa.it. https://orcid.org/0000-0001-8455-8228
Andrea Cipollini, Department of Economics, Business and Statistics, University of Palermo, Viale delle Scienze, 90128 Palermo, Italy, E-mail: andrea.cipollini@unipa.it. https://orcid.org/0000-0002-2272-462X

policymakers to implement the climate policies necessary to meet, in Europe, the 2030 greenhouse gas emissions net reduction intermediate target of 55 % below 1990 levels, and to achieve the long-term European Green Deal target of EU-wide climate neutrality by 2050. In the baseline analysis, we use time series data on air temperature levels and gross value added (GVA) observed for 191 EU NUTS2 regions. The use of sub-national data allows us to account for the within-country heterogeneity in temperatures and growth. The need to avoid aggregation at the country level is motivated by, first, taking into account the exposure of different region units within a country to opposing temperature shocks within a given period and, second, by the wide income differences within countries.[1]

Most of the existing literature on temperature effect on growth has highlighted the role of non-linearities. More specifically, the country-based studies of Burke et al. (2015) and Burke et al. (2018) find an inverted U-shape relationship between temperature and income, and the one by Kahn et al. (2021) find a different impact of positive and negative deviation from a temperature norm proxied by a moving average observed over a long-horizon.[2] Studies based on sub-national data which find evidence of an inverted U-shape relationship between income and temperature are those by Olper et al. (2021) focusing on Italy, and Zhao et al. (2018) using 10,597 global grid cells. The analysis of Greßer et al. (2021), based on sub-national data, does not find evidence of a non-linear (quadratic) effect of temperature on growth. The state-dependent local projection analysis of Nath et al. (2024) based on countrywide annual data shows an impact of temperature on growth conditional on the mean temperature levels. The study of Mohaddes et al. (2023) focus on U.S. states using positive and negative deviation from a temperature norm in a way similar to Kahn et al. (2021). Newell et al. (2021) find a high degree of model uncertainty across specifications differing in terms of non-linearities and lagged temperature effects. The authors suggest, as a future avenue of research, to study the temperature-growth relationship by disaggregating annual temperature data to explore heterogeneous temperature sensitivity across seasons, as well as modelling non-linearities.

Another strand of the literature highlights the role played by seasonal temperature effects. The study of Linsenmeier (2024) focuses on the role played by temperature to seasonal output cycles. The analysis, based on cross-sectional regression (using countrywide data), shows that seasonal differences in temperature between summer and winter have a statistically significant, positive association with seasonal differences in GDP. The unrestricted mixed data sampling (MIDAS) panel regression study of Colacito et al. (2019) focuses on the relationship, for U.S. states, between annual growth and seasonal temperature, while Nguyen (2024) studies the seasonal temperature effect on quarterly employment growth of U.S. municipalities.[3]

Recent studies explore the role of temperature variability on economic growth. Donadelli et al. (2021) and Donadelli et al. (2022) focus on the macroeconomic effects of a temperature anomaly volatility index (defined as the difference between the intra-annual volatility and a benchmark volatility level) on TFP growth for the UK and for a panel of 114 countries, respectively. Kotz et al. (2021) use data for 1537 NUTS2 across global economies to study the effects of temperature variability on economic activity over the 1979 – 2018 time span. The study of Linsenmeier (2023), using cross-sectional regression, examines the effects of day-to-day, seasonal, and interannual temperature variability on long-run economic development. Alessandri and Mumtaz (2025) estimate a structural Panel VAR augmented with stochastic volatility using data for 160 countries observed over the 1961 – 2019 time span, to study the effects of the temperature level or temperature volatility on economic growth.

1 The growth-temperature relationship based on sub-national data is the focus of Deryugina and Hsiang (2014), Colacito et al. (2019), Mohaddes et al. (2023) using data for the U.S. states. Li et al. (2019) focus on Chinese provinces. Olper et al. (2021) focus on NUTS3 data for Italian provinces. The study of Du et al. (2017), Zhao et al. (2018), Acevedo et al. (2020), Kalkuhl and Wenz (2020), and Greßer et al. (2021) use sub-national data for a sample of global economies.

2 De Bandt et al. (2021) focus on a panel of emerging countries and model the non-linearities in the deviation from a temperature norm using a quadratic function.

3 Ciccarelli et al. (2024) use Vector Autoregressions augmented with exogenous variables (VARX) (i.e., measures of temperature-related shocks interacted with seasonal dummies) to study the impact of temperature seasonalities on inflation in four European countries.

The main transmission channel explored in the literature is a supply-side factor such as labour productivity.[4] Some studies (see Acevedo et al. 2020; Donadelli et al. 2017; Fankhauser and Tol 2005) also explore the role played by investments as a transmission channel. The negative effect of a temperature rise on the rate of return on capital could lower the demand for funding investments, and it could also increase the cost of financing investments in the presence of imperfect capital markets. Moreover, several studies (e.g., Acevedo et al. 2020; Groom et al. 2023) have examined whether the impact of temperature on growth differs according to exposure (e.g., the geographical location) and to the level of economic development (proxied by the income per capita of a given country). Finally, some studies (see Kahn et al. 2021; Mohaddes et al. 2023) examine whether there is any evidence of adaptation using rolling estimation of the regression capturing the output-temperature causality relationship.[5]

Our main contribution to the literature on the temperature level-growth relationship is methodological. First, we account for seasonalities and non-linearities jointly. The focus on seasonal temperature is motivated by the Copernicus projections suggesting a rise in temperature over 2020 — 2099, especially during fall-winter, in the absence of climate change mitigation policies. We show that the drivers of a state-dependent local projection of GVA cumulative growth are not only shocks to seasonal temperatures but also their interactions, implying that the marginal effect of each seasonal temperature shock is not only conditional on the global seasonal temperature of a given year but also on idiosyncratic factors such as the seasonal shock in a given region and a given year. Another methodological contribution is given by the use of a mixed-frequency dataset in a non-linear setting and also by the novelty of modelling state-dependent local projections that include non-linear terms in seasonal temperatures (both observed and shocks). We argue that the flexibility of the model proposed allows us to investigate, first, if there is any evidence of adaptation (implicitly) by comparing the full sample estimation results of two regimes: the "no-shock scenario" and the "shock scenario" regime (conditional on 2019 global seasonal averages and on shock observed in 2019 for a median region). Then, since the second stage of the analysis is based only on the "shock scenario" regime (conditional on 2019), we first assess which among labour productivity and investments is the main transmission channel, and then we focus on the main risk mitigation channels (proxied by the state variables considered in the non-linear local projection): exposure to climate risk in terms of geographical location/economic sector and proxies of resilience using either income per capita or an index of regional competitiveness (RCI). The empirical evidence suggests, first, that there is no evidence of adaptation. Furthermore, both labour productivity and, especially, investments play an important role in the transmission mechanism. Finally, construction is one of the most vulnerable sectors, and the regions with a higher income per capita or RCI are the most resilient to temperature shocks. A counterfactual exercise shows that winter and fall are the seasons for which projected temperature increases will be beneficial for GVA growth, especially in cold regions, while the cumulative effect on GVA growth will be negative during spring and summer.

The structure of the paper is organized as follows. Section 2 describes the empirical model. Section 3 describes the empirical analysis: data and empirical findings. Section 4 concludes.

2 Empirical Methodology

We estimate a state-dependent unrestricted mixed data sampling (U-MIDAS) panel local projection where regional GVA growth observed at an annual frequency is regressed onto seasonal (observed and shocks) temperatures. The model specification is along the lines of Nath et al. (2024). In the first stage of the analysis, we focus on the following decomposition of each seasonal temperature ($T_{i,t}^{(s)}$):

4 The impact of temperature on labour productivity also occurs through its impact on human health. While several studies focus on the impact of temperature on excess mortality (see Ballester et al. 2023, among the others), Gibney et al. (2023) use weekly data on morbidity, focusing on accident and emergency (A&E) attendances at 429 hospitals across England from 2010 to 2015. The authors find substantial increases in overall attendance for hotter temperatures.

5 Kahn et al. (2021) and Mohaddes et al. (2023) argue that the country-wide and U.S. evidence of no adaptation should be interpreted with caution given that the transition to a green economy effort might be related only to advanced economies and to specific sectors, and it might have been outpaced by the unprecedented increase in global temperature over the last decades.

$$T_{i,t}^{(s)} = \sum_{j=1}^{p} \rho_j^{(s)} T_{i,t-j}^{(s)} + \sum_{j=1}^{p} \lambda_j^{(s)} T_{i,t-j}^{(s)} \overline{T}_i^{(s)} + \sum_{j=1}^{p} \omega_j^{(s)} T_{i,t-j}^{(s)} \overline{T}_t^{(s)} + \alpha_i + \alpha_t + \tau_{i,t}^{(s)} \tag{1}$$

where $T_{i,t}^{(s)}$ and $\tau_{i,t}^{(s)}$ are the observed temperatures and the innovations hitting region i during season s at year t, respectively. Moreover, $\overline{T}_i^{(s)}$ is the seasonal mean temperature level of each region i (computed across years) and $\overline{T}_t^{(s)}$ is the seasonal mean temperature level of each year t (computed across regions). Finally, α_i and α_t are region- and year-fixed effects. In line with Nath et al. (2024), we allow both for observed persistence in temperature time series and for interactions of the observed lagged temperature with the seasonal mean temperature of each region ($\overline{T}_i^{(s)}$) and the seasonal mean temperature of each year ($\overline{T}_t^{(s)}$). The lag length is set equal to two (i.e., $p = 2$).

In the first stage of the analysis, the OLS estimation of equation (1) allows to retrieve temperature shocks, proxied by the estimated residuals. The focus is, then, on the unanticipated component of temperature to measure the impact on growth.[6] Differently from the study of Nath et al. (2024), we focus on seasonal shocks and we also account for interaction terms between the seasonal temperatures and the seasonal mean temperature level of each year.[7]

The second stage estimation refers to the state-dependent local projection regression in equation (2), using jointly the four time series of residuals (obtained from the estimation of equation (1)) as proxies for the seasonal temperature shocks. More specifically, since data are sampled at a different frequency (i.e., the level of temperature is available at a seasonal frequency, while the proxy of economic activity is sampled annually), we estimate the following state-dependent U-MIDAS panel local projection:[8]

$$\begin{aligned} y_{i,t+h} - y_{i,t-1} = {} & \sum_{s=1}^{4} \beta_s^{(h)} \tau_{i,s,t} + \sum_{s=1}^{4} \eta_s^{(h)} \tau_{i,s,t}^2 + \sum_{\substack{s,r=1 \\ s<r}}^{4} \phi_{s,r}^{(h)} \tau_{i,s,t} \tau_{i,r,t} + \sum_{s=1}^{4} \sum_{r=1}^{4} \theta_{s,r}^{(h)} \tau_{i,s,t} \overline{T}_{i,r} \\ & + \sum_{s=1}^{4} \sum_{r=1}^{4} \gamma_{s,r}^{(h)} \tau_{i,s,t} \overline{T}_{r,t} + \delta'^{(h)} X_{i,t} + \mu_i^{(h)} + \mu_t^{(h)} + \varepsilon_{i,t+h|t-1} \end{aligned} \tag{2}$$

for $h = 0, 1, \ldots, H$ horizons, where $y_{i,t+h} - y_{i,t-1}$ denotes the long differences computed for the proxy of economic activity ($y_{i,t}$), which measures the approximate percentage change in $y_{i,t}$ occurred between $t-1$ and h periods ahead. In equation (2), the dependent variable can be expressed as a function of non-linear terms involving seasonal temperatures, both observed and shocks, together with the linear term ($\tau_{i,s,t}$) and with the control variables and the region- and year-fixed effects. The non-linearities include a quadratic term $\left(\tau_{i,s,t}^2\right)$ and a set of interaction terms: (*i*) the interactions between the seasonal temperature shocks ($\tau_{i,s,t}\tau_{i,r,t}$), (*ii*) the interactions between the seasonal temperature shocks and the seasonal mean temperature level of each region ($\tau_{i,s,t}\overline{T}_{i,r}$), and (*iii*) the interactions between the seasonal temperature shocks and the seasonal mean temperature of each year ($\tau_{i,s,t}\overline{T}_{r,t}$), with $s, r = 1, \ldots, 4$, where the temperature shocks ($\tau_{i,s,t}$) are obtained from the first stage regression. Moreover, the vector of control variables ($X_{i,t}$) includes lags of the observed seasonal temperature series ($T_{i,s,t}$), lags of the seasonal precipitation series ($P_{i,s,t}$), and lags of the growth rate of the annual proxy of economic activity ($\Delta y_{i,t}$). As in equation (1), we set the lag length equal to two (i.e., $p = 2$).[9]

---

6 We acknowledge that our focus on shocks is only on short-run deviation from the conditional mean (function of only two years lags in temperature) and we leave for future research the analysis based on long-term deviation (e.g., from a temperature norm, see Kahn et al. 2021).

7 The evidence of statistically significant coefficients obtained from the estimation of the panel regression in equation (1) points to the importance of including both the interactions with the seasonal mean temperature of each region and with the seasonal mean temperature of each year. The results obtained from the estimation of equation (1) are available upon request.

8 As discussed by Foroni et al. (2015), differently from the restricted MIDAS regressions (see e.g., Ghysels et al. 2007), the unrestricted variant of MIDAS regressions does not rely on functional distributed lag polynomials and, hence, it can be estimated by OLS.

9 See Appendix A for the motivation underlying the non-linear model specification of the panel local projection.

Given the non-linear (e.g., state-dependent) local projection regression, the impulse response profile is obtained from the marginal effects retrieved from the second stage estimation of equation (2). For each horizon, we compute the state-dependent (non-linear) impulse response of the proxy of economic activity to seasonal temperature shocks ($\tau_{i,s,t}$) as follows:

$$\zeta_s^{(h)} = \hat{\beta}_s^{(h)} + 2\hat{\eta}_s^{(h)}\tau_{i,s,t} + \sum_{\substack{r=1 \\ s\neq r}}^{4} \hat{\phi}_{s,r}^{(h)}\tau_{i,r,t} + \sum_{r=1}^{4} \hat{\theta}_{s,r}^{(h)}\overline{T}_{i,r} + \sum_{r=1}^{4} \hat{\gamma}_{s,r}^{(h)}\overline{T}_{r,t} \tag{3}$$

with $\phi_{s,r} = \phi_{r,s}$, which measures the marginal contribution of each of the four seasonal temperature shocks on economic activity. According to equation (3), the marginal effect of seasonal temperature shocks depends not only on the linear and quadratic terms (i.e., the first and second addends in equation (3)), but also on the interactions across seasonal temperatures (both shocks and observed), that is: (*i*) the interactions between the seasonal temperature shocks differing across regions and years (the third set of addends), and (*ii*) the interactions between the seasonal temperature shocks and the average seasonal temperature varying across regions (the fourth set of addends) and years (the fifth set of addends).[10] In line with Bilal and Känzig (2024), our model specification allows the marginal effects in equation (3) to account both for region-specific and global temperature shocks. However, while Bilal and Känzig (2024) focus only on yearly temperature shocks, we consider seasonal temperature shocks and their interactions.

We compute the impulse responses for two regimes. In the first regime, labelled as "no-shock scenario", we assume that no seasonal temperature shocks occur (i.e., we set $\tau_{i,s,t} = 0$, hence we drop the second and third addend of equation (3)), and the average response of GVA is only driven by the level of the seasonal mean temperature computed across regions and time (i.e., the global seasonal averages). More specifically, to compute the average response of regional GVA, we set the seasonal mean temperature of each region ($\overline{T}_{i,s}$) and the seasonal mean temperature of each year ($\overline{T}_{s,t}$) at their average values, that is $\overline{T}_{i,s} = \overline{T}_{s,t} = \text{mean}(T_{i,s,t})$ and these values for winter, spring, summer, and fall are equal to 2.9 °C, 13.1 °C, 17.6 °C, 6.3 °C, respectively. In the second regime, labelled as "shock scenario", we "switch on" the seasonal temperature shocks in equation (3), by setting $\tau_{i,s,t} \neq 0$ and we focus on the median region which is the one having the median temperature value observed across each regional average annual temperatures. In particular, as for the second and third addend in equation (3), we focus on the temperature shock (computed using the estimated residual of equation (1)) to the median region, setting $\tau_{i,s,t} = \tau_{\text{median},s,2019}$ with values for winter, spring, summer, and fall equal to 0.17, −0.21, 0.11, and −0.05, respectively. Moreover, the temperature values entering the fourth addend in equation (3) are equal to the global seasonal averages: 2.9 °C, 13.1 °C, 17.6 °C, 6.3 °C, observed during winter, spring, summer, and fall, respectively. Finally, we use the global seasonal temperature in 2019 (i.e., computing the average across regions in 2019) as the fifth addend in equation (3), with values equal to 4.3 °C, 13.9 °C, 18.5 °C, and 7.8 °C observed during winter, spring, summer, and fall, respectively. We argue that the state-dependent panel local projection model proposed is a new candidate among the hybrid panel models reviewed by Kolstad and Moore (2020) and for which the over-estimation bias of short-run effects arising by not fully accounting for adaptation can be considerably reduced.

Finally, to investigate the importance of seasonal temperature shocks in explaining business cycle fluctuations, we compute the forecast error variance decomposition (FEVD) for the proxy of economic activity. More specifically, we follow Gorodnichenko and Lee (2020) and we compute the FEVD based on the coefficient of determination (R^2) from the local projections. This approach requires two steps. In the first step, we estimate the forecast error ($\hat{f}_{i,t+h|t-1}$) for the proxy of regional economic activity as the residual from the following panel regression:

10 The terms $\overline{T}_{i,r}$ and $\overline{T}_{r,t}$ denote, respectively, the seasonal mean temperature computed for each region (across years) and the seasonal mean temperature computed for each year (across regions).

$$y_{i,t+h} - y_{i,t-1} = \sum_{j=1}^{p}\sum_{s=1}^{4} \delta_{1,s,j}^{(h)} T_{i,s,t-j} + \sum_{j=1}^{p}\sum_{s=1}^{4} \delta_{2,s,j}^{(h)} P_{i,s,t-j} + \sum_{j=1}^{p} \delta_{3,j}^{(h)} \Delta y_{i,t-j} + \mu_i^{(h)} + \mu_t^{(h)} + f_{i,t+h|t-1} \tag{4}$$

that is by regressing the long-differences computed for the proxy of regional economic activity ($y_{i,t}$) onto the lags (i.e., $p = 2$) of seasonal temperatures, seasonal precipitations, and growth rate of the proxy of economic activity (i.e., these correspond to the control variables included in equation (2)). In the second step, for each season, we regress the estimated forecast error ($\hat{f}_{i,t+h|t-1}$) onto the seasonal temperature shock and we compute the R^2:

$$\hat{f}_{i,t+h|t-1} = \varphi_{s,0}\tau_{i,s,t}^{*} + \cdots + \varphi_{s,h}\tau_{i,s,t+h}^{*} + \nu_{i,t+h|t-1} \tag{5}$$

where the seasonal temperature shock entering equation (5) $\left(\tau_{i,s,t+h}^{*}\right)$, for $h = 0, 1, \ldots, H$ is defined as follows:

$$\tau_{i,s,t+h}^{*} = \tau_{i,s,t+h} + \tau_{i,s,t+h}^{2} + \sum_{\substack{r=1\\ s\neq r}}^{4} \tau_{i,s,t}\tau_{i,r,t} + \sum_{r=1}^{4} \tau_{i,s,t}\overline{T}_{i,r} + \sum_{r=1}^{4} \tau_{i,s,t}\overline{T}_{r,t} \tag{6}$$

The FEVD of the proxy of economic activity ($y_{i,t}$) due to seasonal temperature shock $\left(\tau_{i,s,t+h}^{*}\right)$ at each h horizon ($\text{FEVD}_{s,h}^{(y_t)}$) is the R^2 computed by estimating equation (5) for each season, separately.

In the baseline specification, the proxy of real economic activity ($y_{i,t}$) is the (log of) regional real gross value added (GVA).[11] We also consider the following proxies of regional economic activity: (*i*) (log of) real GVA per employee, (*ii*) (log of) gross fixed capital formation, (*iii*) (log of) real GVA by NACE sector. The U-MIDAS panel local projection described in equation (2) is fitted to an unbalanced panel of 191 EU NUTS2 regions, over the period 1980 – 2019.

3 Empirical Analysis

3.1 Data

The state-dependent U-MIDAS panel local projection is estimated using data sampled at a different frequency. More specifically, we use a proxy for seasonal temperature levels and for annual real economic activity, observed for 191 EU NUTS2 regions over the 1980 – 2019 time span.[12] In the baseline specification, we use data on GVA at constant prices (deflated to 2015 price levels) as a measure of real economic activity. The data are collected from the publicly available Annual Regional Database of the European Commission's (ARDECO database) Directorate General for Regional and Urban Policy, which is maintained and updated by the Joint Research Centre.[13] As explained in the Introduction, among the transmission channels, we consider the contribution of different sectors to the effect of temperature on GVA. For this purpose, we estimate the state-dependent U-MIDAS panel local projection using data for GVA at constant prices disaggregated into six NACE2 sectors: (*i*) agriculture, forestry and

11 Data on real gross domestic product (GDP) is also available in the ARDECO database. However, we prefer to use real GVA as a proxy for real economic activity whose data is also available for the different economic sectors. Results for real GDP are qualitatively and quantitatively similar to those obtained using the aggregate real GVA and they are available upon request.

12 Although data on temperature levels and economic activity are available up to 2021 for most of the regions included in the sample, we prefer to exclude the COVID-19 observations and estimate the models using data up to 2019.

13 The database contains information on demographic and macroeconomic (including labour market, capital formation and domestic product) variables for the EU27 countries plus Albania (AL), Montenegro (ME), North Macedonia (MK), Norway (NO), Serbia (RS), and Turkey (TR). Data are available for all the levels of the Nomenclature of territorial units for statistics (NUTS), that is NUTS0 (corresponding to the country level), NUTS1, NUTS2 and NUTS3 (i.e., the lowest level of the territorial classification). The time series cover the period 1980 – 2023, where the last four annual observations are forecasted based on the 2017 – 2019 trend. Data and technical details can be found on the ARDECO online page.

fishing, (*ii*) industry, excluding construction, (*iii*) construction, (*iv*) wholesale, retail, transport, accommodation and food services, information and communication (in the following referred to as wholesale), (*v*) financial and business services, and (*vi*) non-market services.[14] Moreover, to investigate the labour productivity and investment transmission channels, we also estimate the U-MIDAS panel local projection by using the GVA to employees ratio (as a proxy for labour productivity) and the gross fixed capital formation (as a proxy for investment).[15]

In our study, the main climate variable is the level of the monthly average temperature. As a control variable in the U-MIDAS panel local projection, we also use the level of monthly precipitation. Both the climate variables are registered during four seasons, i.e., winter (January, February, and March), spring (April, May, and June), summer (July, August, and September), and fall (October, November, and December).[16] More specifically, for both temperature and precipitation, we use monthly NUTS2-level data downloaded from the Copernicus Climate Change Service (2020) operational energy dataset.

The database contains climate-relevant indicators for the energy sectors, such as air temperature, among others, for 38 European countries from 1979 onward.[17] The historical dataset produces reference climate variables based on the European Centre for Medium-Range Weather Forecasts (ECMWF) Reanalysis fifth generation (ERA5) and retrieved from the Climate Data Store. Data are available both at the grid (approximately 30 × 30 km) and at the country (NUTS0) and regional (NUTS2) levels.[18] In our empirical application, as for the level of temperature, we use the 2 m air temperature series, which is defined as the ambient air temperature near to the surface (i.e., typically at a height of 2 m). We collect the monthly (averaged) series for NUTS2 regions and we compute the seasonal temperatures by averaging out the observations across the three months. The series of temperatures are measured in degrees Kelvin (K). We convert the series into degrees Celsius (°C). As for the level of precipitation, we use the total precipitation measured in metres (m). The series of seasonal precipitation are computed by summing up the monthly observations for NUTS2 regions over three months.

The final dataset includes regional observations of temperature levels, precipitation, and real GVA for 16 EU countries and it is constructed as follows.[19] First, we exclude from the initial sample of 33 countries (that is the maximum geographical coverage for which information on both economic activity and temperature is available) the ones that consist of only one NUTS2 region (i.e., no distinction between NUTS levels): Cyprus, Estonia, Luxembourg, Latvia, Montenegro, North Macedonia, and Malta. Moreover, Albania, Norway, Serbia, and Turkey are excluded since they are not EU members. Furthermore, we exclude the NUT2 regions of Bulgaria, Greece, Croatia, Ireland, Lithuania, and Romania, whose time series of sectoral GVA report more than 15 missing observations.[20] Finally, since data on 2 m air temperature and precipitation are not available for *Région de Bruxelles-Capitale* (BE10), *Bremen* (DE50), *Ciudad Autónoma de Ceuta* (ES63), *Ciudad Autónoma de Melilla* (ES64), *Guadeloupe* (FRY1), *Martinique* (FRY2), *Guyane* (FRY3), *La Réunion* (FRY4), *Mayotte* (FRY5), and Região Autónoma dos Açores (PT20), we remove these regions from the estimation sample.

14 The ARDECO data of the non-market services sector include government consumption in the following sub-sectors: (*i*) Public administration and defence; (*ii*) Education; (*iii*) Human health and social work; (*iv*) Arts, entertainment, and recreation; (*v*) Other service activities; (*vi*) Activities of households and extra-territorial organizations and bodies.

15 The source of both the number of employees and the gross fixed capital formation is ARDECO.

16 See Colacito et al. (2019) for a similar construction of seasonal temperature proxies.

17 Data are available for Albania (AL), Austria (AT), Bosnia and Herzegovina (BA), Belgium (BE), Bulgaria (BG), Switzerland (CH), Cyprus (CY), Czech Republic (CZ), Germany (DE), Denmark (DK), Estonia (EE), Greece (EL), Spain (ES), Finland (FI), France (FR), Croatia (HR), Hungary (HU), Ireland (IE), Island (IS), Italy (IT), Lichtenstein (LI), Lithuania (LT), Luxembourg (LU), Latvia (LV), Montenegro (ME), North Macedonia (MK), Malta (MT), Netherlands (NL), Norway (NO), Poland (PL), Portugal (PT), Romania (RO), Serbia (RS), Sweden (SE), Slovenia (SI), Slovakia (SK), Turkey (TR), and United Kingdom (UK).

18 The "Climate and energy indicators for Europe from 1979 to present derived from reanalysis" database is updated at a monthly frequency and it is available at the Copernicus Climate Data Store online page.

19 The 16 EU countries are Austria (AT), Belgium (BE), Czech Republic (CZ), Germany (DE), Denmark (DK), Spain (ES), Finland (FI), France (FR), Hungary (HU), Italy (IT), Netherlands (NL), Poland (PL), Portugal (PT), Sweden (SE), Slovenia (SI), and Slovakia (SK). In the baseline specification, we deal with an unbalanced panel of observations given that data availability differs both between and within countries, especially for macroeconomic data.

20 The results obtained by including the observations for the regions of these six countries (i.e., those reporting more than 15 missing observations in the sectoral GVA series) in the estimation sample remain qualitatively similar and they are available upon request.

Table 1: Descriptive statistics.

Variable		NUTS	N. obs	Mean	Median	Min	Max	Std. dev.
Temperature (°C)	Winter	191	7,640	2.92	3.03	−15.75	17.36	4.18
	Spring	191	7,640	13.08	13.03	1.03	20.70	2.65
	Summer	191	7,640	17.58	17.23	7.80	26.43	2.82
	Fall	191	7,640	6.32	6.07	−8.34	19.43	3.70
Precipitation (m)	Winter	191	7,640	0.19	0.18	0.02	0.98	0.09
	Spring	191	7,640	0.23	0.21	0.01	0.72	0.09
	Summer	191	7,640	0.22	0.22	0.00	0.70	0.10
	Fall	191	7,640	0.23	0.21	0.04	0.88	0.10
ΔGVA (%)		191	6,945	1.88	1.95	−26.08	48.20	3.37

Notes: Descriptive statistics for the series of seasonal temperatures, seasonal precipitations, and annual aggregate real GVA growth rate, observed for 191 NUTS2 regions over the period 1980−2019. Seasonal temperatures are measured in degrees Celsius (°C), seasonal precipitations are measured in metres (m), and real GVA growth rate is expressed in percent.

Table 1 shows summary statistics for the levels of seasonal temperature and seasonal precipitation as well as for the growth rate of real GVA, over the period 1980 − 2019. The average values of the four seasonal temperature level series are equal to 2.92 °C (winter), 13.08 °C (spring), 17.58 °C (summer), and 6.32 °C (fall). The season reporting the largest standard deviation is winter (4.18 °C), while the smallest standard deviation is reported by spring (2.65 °C). The average values of the level of precipitation (ranging from 0.19 m to 0.23 m), as well as their standard deviations (ranging from 0.09 m to 0.10 m), are similar across the four seasons. As for the real GVA growth, the average value is equal to 1.88 %, while the standard deviation is equal to 3.37 %.

To investigate whether the temperature levels increased in the 191 NUTS2 regions over the 1980 − 2019 period, we follow Kahn et al. (2021) and Mohaddes et al. (2023) and we regress the temperature levels on a

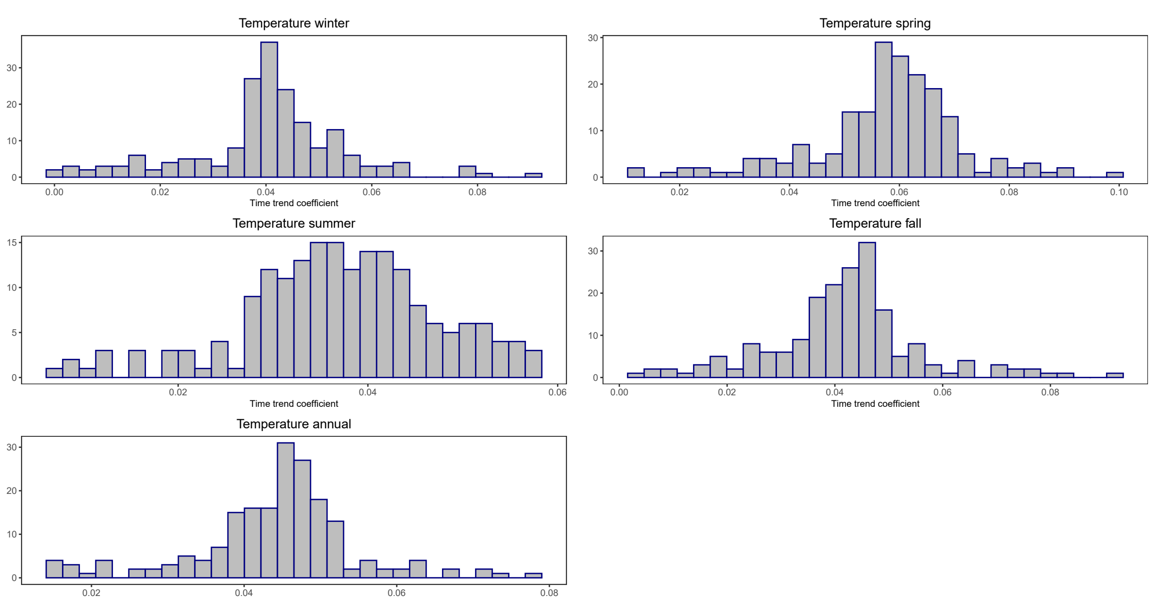

Figure 1: Estimates of the average increase in temperature levels over the 1980 − 2019 time period. Notes: Empirical distribution of the estimate of the coefficients associated with the deterministic time trend (β_i) of the following regression: $T_{i,t} = \alpha_i + \beta_i t + u_{i,t}$, where $T_{i,t}$ is the temperature levels observed in each of four seasons individually (winter, spring, summer, and fall) and the averaged yearly temperature observed for the i-th NUTS2 region.

constant term and a deterministic linear time trend for each NUTS2 region.[21] The region-specific coefficients associated with the time trend, which measure to what extent the temperature has increased on average per year, are reported in Figure 1. We report the results for the seasonal temperatures as well as for the annual (averaged) temperature. As can be seen in Figure 1, temperature levels observed in each season increased over the 1980 – 2019 time span, in almost all the NUTS2 regions. The largest average (across NUTS2 regions) per annum increase in temperature levels has been observed in spring (0.058 °C), followed by fall (0.042 °C), winter (0.040 °C), and summer (0.037 °C), while the average (across NUTS2) rise in annual temperature is equal to 0.044 °C per annum.

Table 2 (Panel A) shows the contemporaneous correlation of temperatures observed (on average) between different seasons. The observed high contemporaneous correlation, within a year, between temperature levels of different seasons suggests that it cannot be ignored the role played, individually and jointly, by seasonal temperature in a given year and a given region (see the evidence in Table 2, Panel B, of statistically significant coefficients for interaction terms in a static regression of GVA growth on the observed seasonal temperatures). Finally, the empirical evidence points to a better fit of the non-linear mixed-frequency model specification than the one of a non-linear common-frequency model (see Appendix B for details).

Table 2: Seasonal temperatures interactions.

Panel A: Contemporaneous correlation					
		T_{winter}	T_{spring}	T_{summer}	T_{fall}
	T_{winter}	1	0.74	0.73	0.87
	T_{spring}	–	1	0.87	0.76
	T_{summer}	–	–	1	0.79
	T_{fall}	–	–	–	1
Panel B: Panel regression. *Dep. variable* ΔGVA					
		Winter	Spring	Summer	Fall
ΔGVA	T_s	0.11	−0.10	0.31	−0.37
		(0.22)	(0.32)	(0.47)	(0.38)
	T_s^2	0.02**	0.08***	0.02	−0.02
		(0.01)	(0.02)	(0.02)	(0.01)
	$T_{\text{winter}} \times T_s$	–	−0.05***	0.02	0.02
		(–)	(0.02)	(0.02)	(0.02)
	$T_{\text{spring}} \times T_s$	–	–	−0.09***	−0.03
		(–)	(–)	(0.03)	(0.02)
	$T_{\text{summer}} \times T_s$	–	–	–	0.05
		(–)	(–)	(–)	(0.03)

Notes: The figure shows two panels. Panel A shows the contemporaneous correlation coefficients computed across the seasonal temperature levels. Each series of seasonal temperatures is obtained by pooling the observations across the 191 NUTS2 regions over the 1980–2019. Panel B shows the estimated coefficients (in percent) from the following panel regression: $\Delta y_{i,t} = \sum_{s=1}^{4} \beta_s T_{i,s,t} + \sum_{s=1}^{4} \eta_s T_{i,s,t}^2 + \sum_{\substack{s,r=1 \\ s<r}}^{4} \phi_{s,r} T_{i,s,t} T_{i,r,t} + \mu_i + \mu_t + \varepsilon_{i,t}$, where $y_{i,t}$ is the logarithm of real GVA, $T_{i,s,t}$ is the seasonal temperature series, with $s =$ winter, spring, summer, fall, and μ_i and μ_t are region- and year-fixed effects. The coefficients in the first row of Panel B are those associated with the first four addends (linear terms) of the aforementioned panel regression; the coefficients in the second row of Panel B are those associated with the second four addends (quadratic terms); and the coefficients in the last three rows of Panel B are those associated with the interaction terms. The total number of observations is equal to 6,945, while the R^2 is equal to 0.31. Standard errors clustered by region are reported in brackets. Estimation sample 1980–2019. ***p-value < 0.01, **p-value < 0.05, *p-value < 0.1.

21 As in Kahn et al. (2021) and Mohaddes et al. (2023), the region-specific regression has the following representation: $T_{i,t} = \alpha_i + \beta_i t + u_{i,t}$, where $T_{i,t}$ is the temperature levels observed in region i at year t. While Kahn et al. (2021) and Mohaddes et al. (2023) focus only on the annual average, we also consider each season individually. Moreover, β_i is the region-specific coefficient associated with the linear time trend and it measures the per annum average rise in temperature levels reported by the i-th region.

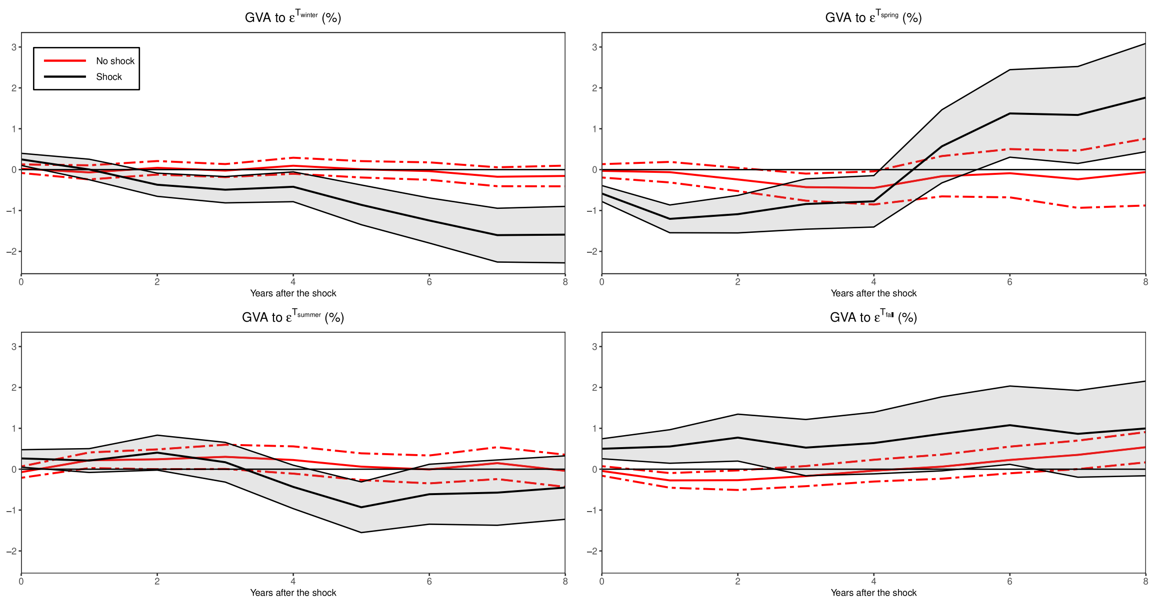

Figure 2: Average response of real economic activity in EU. Notes: Impulse response of the level of real aggregate GVA to seasonal temperature shocks (in percent) computed over an eight-year forecast horizon. The charts show the impulse response profile of GVA to temperature shocks occurring in winter $\left(\varepsilon^{T}_{\text{winter}}\right)$, spring $\left(\varepsilon^{T}_{\text{spring}}\right)$, summer $\left(\varepsilon^{T}_{\text{summer}}\right)$, and fall $\left(\varepsilon^{T}_{\text{fall}}\right)$. Each chart displays the impulse response computed for two scenarios (see equation (3) for more details on how to compute impulse response). As for the "no-shock scenario" (point estimates reported in red solid line), the impulse responses are obtained by setting $\tau_{i,s,t} = 0$ and $\overline{T}_{i,s} = \overline{T}_{s,t} = \text{mean}(T_{i,s,t})$, for $s = 1, \ldots, 4$. For each season, the mean temperature levels computed across regions and years, i.e., $\text{mean}(T_{i,s,t})$, are equal to, respectively, 2.9 °C (winter), 13.1 °C (spring), 17.6 °C (summer), 6.3 °C (fall). As for the "shock scenario" (point estimates reported in black solid line), the impulse responses are obtained by setting $\tau_{i,s,t} = \tau_{\text{median},s,2019}$, i.e., the seasonal shocks hitting the "median" region (i.e., the one whose average historical annual temperature corresponds to the median of the empirical distribution of temperature) in 2019. The "median region" is Karlsruhe (DE12) and the associated shocks are equal to 0.17 (winter), −0.21 (spring), 0.11 (summer), and −0.05 (fall), respectively. Moreover, the impulse response for the "shock scenario" are computed by setting the following values for the annual seasonal temperature of each region and of each year: (*i*) $\overline{T}_{i,s} = \text{mean}(\overline{T}_{i,s})$, which are equal to, respectively, 2.9 °C (winter), 13.1 °C (spring), 17.6 °C (summer), 6.3 °C (fall); (*ii*) $\overline{T}_{s,t} = \text{mean}(\overline{T}_{s,2019})$, which are equal to, respectively, 4.3 °C (winter), 13.9 °C (spring), 18.5 °C (summer), 7.8 °C (fall). The 90 % confidence intervals based on clustered (by region) standard errors are reported for both the "no-shock" (red dashed lines) and "shock" (grey shadow area) scenarios. The size of the temperature shocks in each season is equal to 1 °C increase in the temperature levels, for both the two scenarios. Estimation sample: 1980 − 2019.

3.2 Seasonalities and Non Linearities: Aggregate Results

In this Section, we first observe if there is any evidence of adaptation (implicitly) by comparing full sample estimation results of the two regimes: "no-shock scenario" and "shock scenario" (the latter conditional on 2019, i.e., on the values of the average global temperature in 2019 and on the shock hitting the "median" region in 2019) as described in Section 2. Figure 2 shows the average impulse responses of the level of real GVA to temperature shocks (ε^{T}) in each of the four seasons (i.e., winter, spring, summer, and fall), using the 1980 − 2019 period as estimation sample.[22]

For each season, the impulse response profile for the level of GVA is obtained by computing the marginal contribution of temperature shock using the coefficients estimated from the panel local projection on the long-difference computed for GVA (see equation (3)). This corresponds to computing the cumulative sum of the per-period percentage changes. For both scenarios, we report the 90 % confidence intervals obtained by clustering

22 The estimated coefficients of the local projection regression, on impact, reported in Table B.1 (see Appendix B), support the inclusion of the interaction terms involving seasonal temperature shocks (and observed seasonal temperature) in the proposed state-dependent U-MIDAS panel local projection. The empirical model and findings show evidence of a significant contribution from both regional and European-wide temperature effects on GVA growth.

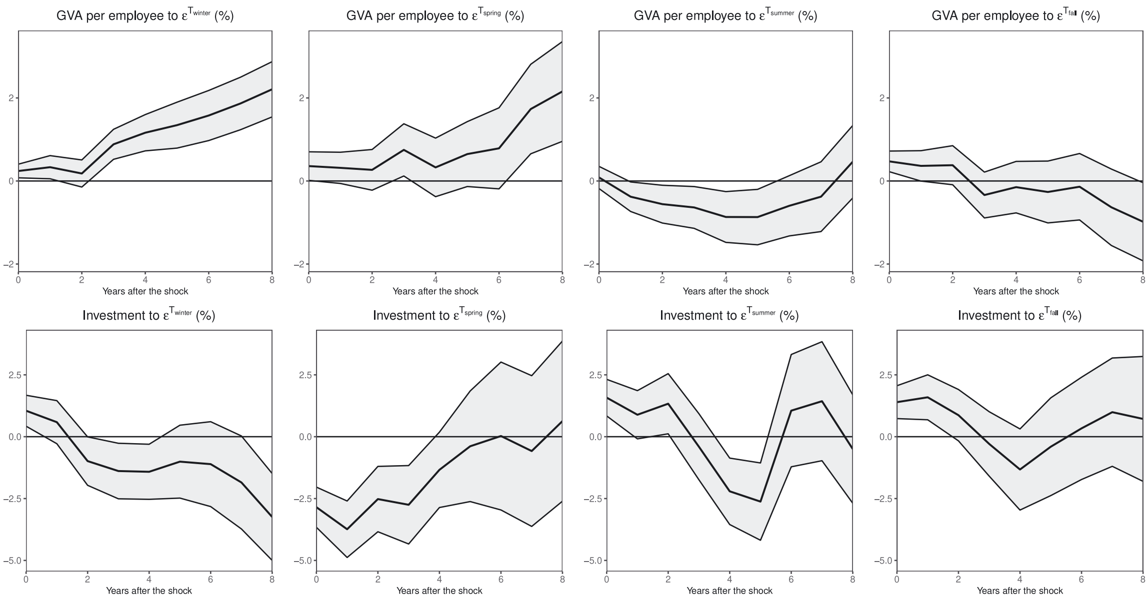

Figure 3: Average response of labour productivity and investment in EU. Notes: Impulse response of the level of real aggregate GVA per employee (upper panel) and gross fixed capital formation (investment) (lower panel) to seasonal temperature shocks (in percent) computed over an eight-year forecast horizon. The charts show the impulse response profile of GVA per employee and investment to temperature shocks occurring in winter $\left(\varepsilon^{T}_{\text{winter}}\right)$, spring $\left(\varepsilon^{T}_{\text{spring}}\right)$, summer $\left(\varepsilon^{T}_{\text{summer}}\right)$, and fall $\left(\varepsilon^{T}_{\text{fall}}\right)$. Each chart displays the impulse response computed for the "shock scenario". For more details on how to compute the impulse responses for the "shock scenario", see the notes in Figure 2. The 90 % confidence intervals based on clustered (by region) standard errors are reported (grey shadow area). The size of the temperature shocks in each season is equal to 1 °C increase in the temperature levels. Estimation sample: 1980 – 2019.

the standard errors by region: the red dashed line is for the "no shock scenario", while the grey shadow area is for the "shock scenario". Finally, the size of the temperature shock in each season is equal to a 1 °C rise in the level of seasonal temperature on impact (i.e., a unitary increase in the temperature level in each of the four seasons) and they are computed over an eight-year forecast horizon.[23]

Figure 2 gives evidence of a statistically significant cumulative impact of temperature on economic activity only under the "shock scenario" regime showing a positive effect during fall (which is equal to 0.76 % on average over an eight-year horizon) and a negative one during winter and spring (with negative peak equal to −1.6 % and −1.2 %, respectively), while summer exhibits a statistically significant negative effect only over a five-year horizon (the negative peak is at horizon five and it is equal to −0.93 %). The comparison of the "shock scenario" regime (conditioning on 2019) with the "no-shock scenario" regime capturing the response of output to temperature averaged over 1980 – 2019, suggests, in line with a number of authors (see the rolling estimation results of the ARDL model fitted to a large panel of countries by Kahn et al. 2021, among the others) a weak adaptation to climate change.

We now examine the role played by main transmission channels and since the focus is on the 2019 "shock scenario" regime, the analysis is on the main channels of climate risk mitigation. We, first, explore the role played by labour productivity (proxied by GVA per employee) and investments (proxied by gross fixed capital formation) in shaping the response of GVA cumulative growth to a temperature rise. Figure 3 shows the response of labour productivity and investment to seasonal temperature shocks in the upper and lower panel, respectively. Inspection of Figure 3 shows that labour productivity benefits from a temperature rise during winter and

23 A panel local projection of the observed seasonal temperatures onto the seasonal temperature shocks, both linear ($\tau_{i,s,t}$) and quadratic $\left(\tau^2_{i,s,t}\right)$ terms, and the interactions of the seasonal temperature shocks with the seasonal mean temperature of each region ($\overline{T}_{i,s}$) and year ($\overline{T}_{s,t}$) shows a response of the seasonal temperature level equal to 1 °C on impact, in both the two scenarios. Results for each season are available upon request.

that investment is the main driver of the reduction in the GVA cumulative growth observed during winter and spring and of the GVA increase during fall. Our empirical evidence is in line with the study of Acevedo et al. (2020) based on the estimation of a panel regression fitted to sub-national data analyzing quadratic temperature effect on growth.

We further examine the role played by geographical vulnerability by discriminating between hot and cold regions. The former are those showing an average annual temperature below (or equal to) 9.7 °C, which is the median of the overall temperature empirical distribution, while the latter are those reporting an average annual temperature above the median of the overall temperature empirical distribution. Figure 4 shows, for hot regions, a short-term positive effect during fall and a decrease in cumulative GVA growth in hot regions during summer (−3.18 %) and winter (−3.81 %), limited to the first two years during spring. Cold regions benefit from a temperature increase in winter and summer (the cumulative response over an eight-year horizon is equal to 0.77 % and 1.43 %, respectively). During fall, a rising temperature has beneficial effects on hot regions (the average response across the eight-year horizon is equal to 1.93 %), while cold regions respond negatively over the whole forecast horizon. Overall, there is evidence of an inverted U-shape (i.e., a beneficial effect in cold regions and a detrimental one for hot regions) especially during summer and, to a lesser extent, during winter and spring.

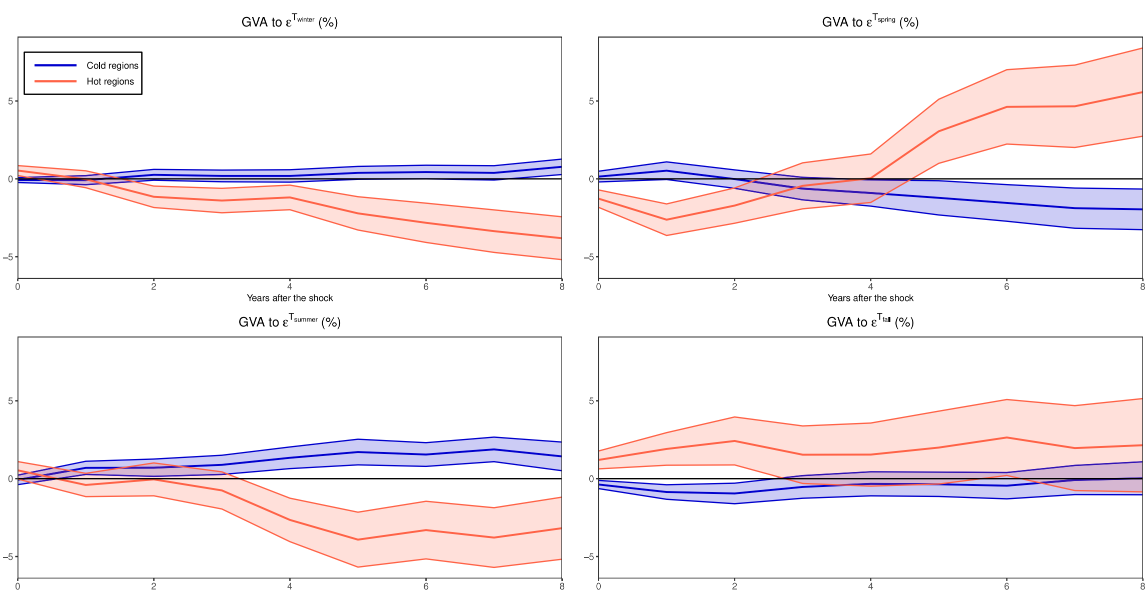

Figure 4: Response of real economic activity in hot and cold regions. Notes: Impulse response of the level of real aggregate GVA to seasonal temperature shocks (in percent) for cold (point estimates reported in blue solid line) and hot (point estimates reported in red solid line) NUTS2 regions, computed over an eight-year forecast horizon. The charts show the impulse response profile of GVA to temperature shocks occurring in winter $(\varepsilon^T_{\text{winter}})$, spring $\left(\varepsilon^T_{\text{spring}}\right)$, summer $(\varepsilon^T_{\text{summer}})$, and fall $(\varepsilon^T_{\text{fall}})$. Each chart displays the impulse response computed for the "shock scenario". A region is labelled as a cold region if its annual temperature (averaged across 1980 − 2019) is lower or equal to the median of the temperature empirical distribution (9.7 °C), while a region is labelled as a hot region if its annual temperature (averaged across 1980 − 2019) is greater than the median of the temperature empirical distribution. For each season, the impulse responses are obtained by setting the shocks $(\tau_{i,s,t})$ as well as the seasonal mean temperature of each region $(\overline{T}_{i,s})$ and the one of each year $(\overline{T}_{s,t})$ at their mean values computed across each subgroup (i.e., cold and hot regions). More specifically, as for cold regions, the conditioning values are set as follows: (*i*) $\tau_{i,s,t} = \text{mean}(\tau_{\text{cold},s,2019})$, i.e., 0.4 (winter), 0.4 (spring), −0.1 (summer), and 0.2 (fall); (*ii*) $\overline{T}_{i,s} = \text{mean}(\overline{T}_{\text{cold},s})$, i.e., 0.3 °C (winter), 11.6 °C (spring), 15.8 °C (summer), and 3.9 °C (fall); (*iii*) $\overline{T}_{s,t} = \text{mean}\left(\overline{T}^{\text{cold}}_{s,2019}\right)$, i.e., 2 °C (winter), 12.7 °C (spring), 16.7 °C (summer), and 5.6 °C (fall). As for hot regions, the conditioning values are set as follows: (*i*) $\tau_{i,s,t} = \text{mean}(\tau_{\text{hot},s,2019})$, i.e., −0.4 (winter), −0.4 (spring), 0.1 (summer), and −0.2 (fall); (*ii*) $\overline{T}_{i,s} = \text{mean}(\overline{T}_{\text{hot},s})$, i.e., 5.6 °C (winter), 14.6 °C (spring), 19.3 °C (summer), and 8.7 °C (fall); (*iii*) $\overline{T}_{s,t} = \text{mean}\left(\overline{T}^{\text{hot}}_{s,2019}\right)$, i.e., 6.7 °C (winter), 15 °C (spring), 20.3 °C (summer), and 10 °C (fall). The 90 % confidence intervals based on clustered (by region) standard errors are reported for both cold (blue shadow area) and hot (red shadow area) regions. The size of the temperature shocks in each season and both for cold and hot regions is equal to 1 °C increase in the temperature levels. Estimation sample: 1980 − 2019.

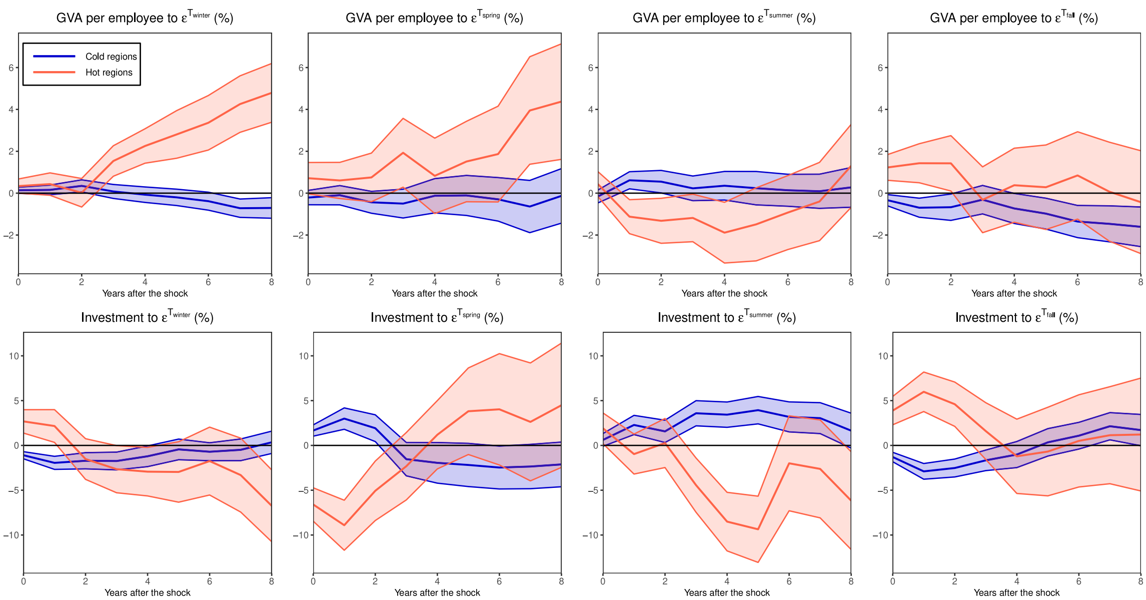

Figure 5: Responses of labour productivity and investment in hot and cold regions. Notes: Impulse response of the level of real aggregate GVA per employee (upper panel) and gross fixed capital formation (investment) (lower panel) to seasonal temperature shocks (in percent), for cold (point estimates reported in blue solid line) and hot (point estimates reported in red solid line) NUTS2 regions, computed over an eight-year forecast horizon. The charts show the impulse response profile of GVA per employee and investment to temperature shocks occurring in winter $\left(\varepsilon^T_{\text{winter}}\right)$, spring $\left(\varepsilon^T_{\text{spring}}\right)$, summer $\left(\varepsilon^T_{\text{summer}}\right)$, and fall $\left(\varepsilon^T_{\text{fall}}\right)$. Each chart displays the impulse response computed for the "shock scenario". For more details on how to compute the impulse responses for both the cold and hot regions, see the notes in Figure 4. The 90 % confidence intervals based on clustered (by region) standard errors are reported for both cold (blue shadow area) and hot (red shadow area) regions. The size of the temperature shocks in each season and both for cold and hot regions is equal to 1 °C increase in the temperature levels. Estimation sample: 1980 — 2019.

An inspection of Figure 5 suggests the following evidence for the impact of temperature on labour productivity and investment. As shown in Figure 5, summer is the only season where we observe a clear contribution of both transmission channels on the asymmetries in the response of GVA. As for labour productivity, hot regions are negatively affected by rising temperature (the average response over the whole forecast horizon is equal to −0.73 %), while cold regions benefit from higher temperatures in summer (0.26 % is the average response over the eight-year horizon). The investment channel also plays an important role in explaining the asymmetric response of GVA observed in summer: hot regions experience a large reduction in investment due to temperature shocks (−3.54 % on average over the eight-year horizon), while we find a beneficial effect for colder regions (2.59 % on average over the eight-year horizon). Likewise, the asymmetric response in GVA observed in fall (positive response for hot regions and negative response for cold regions) can be ascribed to both transmission channels. As for the other seasons, the evidence is more mixed. Whilst in spring the reduction (increase) of GVA for hot (cold) regions is driven by the impulse response profile of investment, for winter none of the transmission channels can explain the asymmetric response of GVA between hot and cold regions.

Overall, the empirical findings suggest, either for the whole EU or for hot and cold regions, that investments are the main driver of the GVA growth response to seasonal temperature shocks.

3.3 Seasonalities and Non Linearities: Sector Contribution

In this Section, we disentangle the geographical vulnerability channel, by discriminating between the most exposed sectors (i.e., agriculture, industry and construction) versus services in each group of regions (hot and cold) (see Figure 6). As shown by Figure 6 (Panel A), during winter, positive effects are limited to agriculture in cold regions and, during this season, the sectors showing, in hot regions, major losses are agriculture, industry

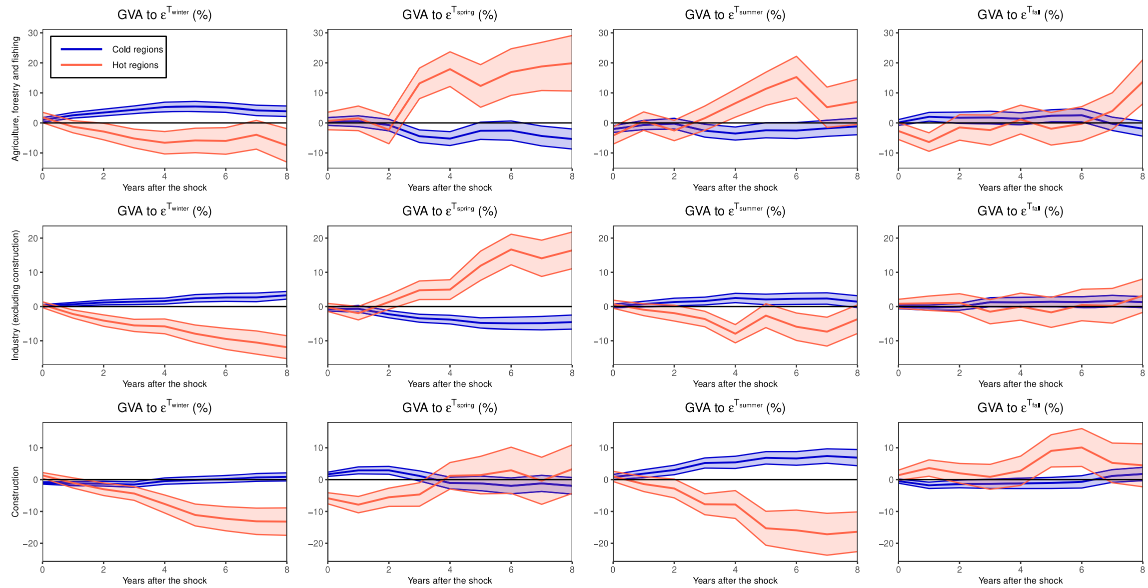

(a)

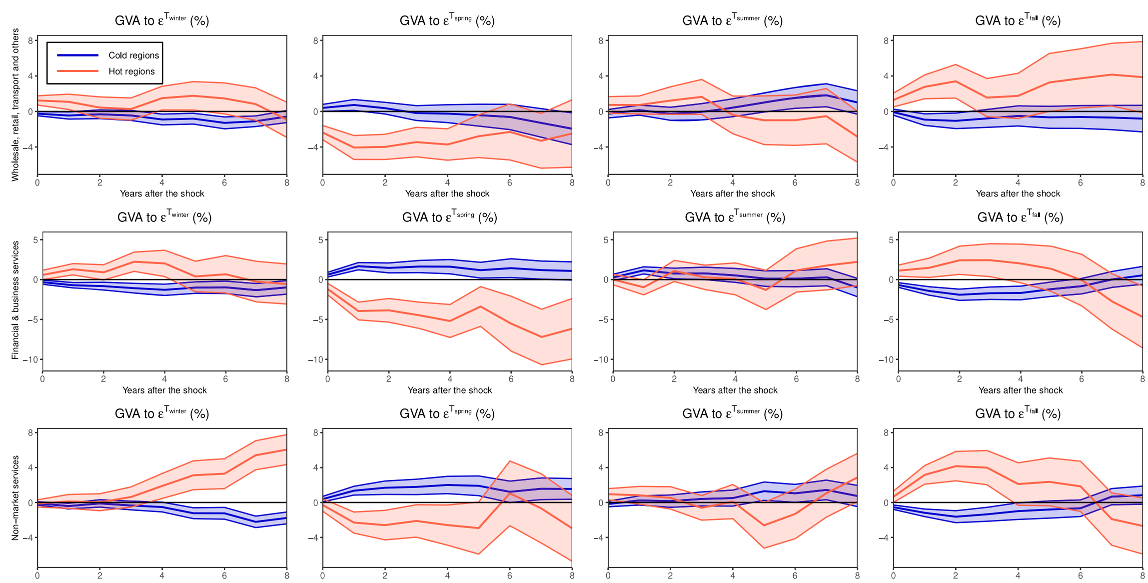

(b)

Figure 6: Response of GVA for different economic sectors in cold and hot NUTS2 regions. (a) Agriculture, forestry and fishing; industry (excluding construction); construction. (b) Wholesale, retail, transport, accommodation and food services, information and communication; financial & business services; non-market services. Notes: Impulse response of the level of real GVA for different NACE sectors to seasonal temperature shocks (in percent), for cold (point estimates reported in blue solid line) and hot (point estimates reported in red solid line) NUTS2 regions, computed over an eight-year forecast horizon. The charts show the impulse response profile of GVA for different NACE sectors to temperature shocks occurring in winter $\left(\varepsilon^T_{\text{winter}}\right)$, spring $\left(\varepsilon^T_{\text{spring}}\right)$, summer $\left(\varepsilon^T_{\text{summer}}\right)$, and fall $\left(\varepsilon^T_{\text{fall}}\right)$. Each chart displays the impulse response computed for the "shock scenario". For more details on how to compute the impulse responses for both the cold and hot regions, see the notes in Figure 4. The 90 % confidence intervals based on clustered (by region) standard errors are reported for both cold (blue shadow area) and hot (red shadow area) regions. The size of the temperature shocks in each season and both for cold and hot regions is equal to 1 °C increase in the temperature levels. Estimation sample: 1980 – 2019.

and construction. Summer is beneficial for agriculture in hot regions and, during this season, major losses are observed in industry and construction. Spring is beneficial for agriculture and industry in hot regions and, to some extent, over a short horizon, for construction in cold regions. The largest negative effects during spring are observed for the construction sector in hot regions. Fall shows a positive effect on construction and a negative one on agriculture. Overall, there is evidence, during winter, of an inverted U-shape relationship between temperature and growth for the most exposed sectors: the cumulative GVA growth in agriculture over an eight-year horizon is equal to 3.88 % and −7.49 % for cold and hot regions, respectively; the cumulative GVA growth in industry is equal to 3.29 % and −11.88 % in cold regions and hot regions, respectively; the cumulative GVA growth in construction is equal to 0.86 % and −13.19 % in cold regions and hot regions, respectively. There is evidence of an inverted U-shape during summer only for industry and construction: the cumulative GVA growth in industry is equal to 1.42 % in cold regions and to −3.69 % in hot regions; the cumulative GVA growth in construction is equal to 6.90 % in cold regions and to −16.38 % in hot regions. Spring and fall show less evidence of an inverted U-shape limited, over a short-term horizon, to construction and agriculture, respectively.

As for services (see Figure 6, Panel B), the evidence of an inverted U-shape is limited only to spring and for the financial & business services sector (the cumulative gains and losses in cold and hot regions are equal to 1.08 % and −6.16 %, respectively) and for non-market services sector (the cumulative gains and losses in cold and hot regions are equal to 1.55 % and −2.96 %, respectively). Evidence of a U-shape relationship between temperature and GVA is observed during winter and fall: while all three service sectors of hot regions benefit from an increase in temperature, there is evidence of a detrimental effect in cold regions. The evidence of a reduction in the output of services sectors observed for cold regions during winter and fall is in line with the empirical findings shown by Groom et al. (2023) for Europe. In particular, the authors argue that rising temperatures in cold regions can affect the opportunity costs of work versus leisure and the working hours for activities that take place typically indoors (such as the services sector).[24]

Table 3 shows the FEVD estimation results for aggregate GVA, GVA per employee, and investment. Temperature contributes the most to cumulative growth over a horizon at most equal to two years during winter and fall (4.87 % and 2.91 %, respectively). Winter and summer are the seasons during which temperature contributes the most to cumulative growth over a longer-term (eight-year) horizon (13.73 % and 11.82 %). Labour productivity and investment contribute in a similar way especially during spring (3.34 % and 3.70 %, respectively) and summer (3.27 % and 3.16 %, respectively) over a short-term horizon, at most equal to two years. Table 3 suggests a more relevant contribution of the investment channel than labour productivity over a long-term horizon (eight years), especially during winter (20.03 % vs. 12.66 %). Spring is the only season during which the FEVD suggests a slightly more relevant contribution of labour productivity than investment over a long-term horizon (14.20 % vs. 13.56 % over an eight-year forecast horizon).

An inspection of Table 4 shows that the primary and secondary sectors are those mostly exposed to a temperature shock during winter: the FEVD at horizon zero of agriculture, industry and construction GVA is equal to 0.99 %, 1.09 % and 0.92 %, respectively and these figures are larger than the corresponding ones for the services sector. Temperature shocks to the construction sector explain the largest contribution of the variability of cumulative growth of GVA over a long-term horizon in each season, especially during winter and summer (25.36 % and 19.51 %, respectively). This empirical finding suggests that construction is one of the most exposed (vulnerable) economic sectors to rising temperature shocks.

3.4 Income Per Capita, Regional Competitiveness and Seasonal Effects

Since the seminal study of Dell et al. (2012), finding that higher temperatures substantially reduce economic growth in poor countries, a number of studies have analyzed the heterogeneous (according to income group) impact of temperature on growth. Recently, Kahn et al. (2021) find that, although weather shocks have a large

24 As for the relationship between temperature and services, see also the study by Falk and Lin (2018) showing a negative (but decreasing since the early 1990s) impact of temperatures on tourism demand in the winter season in the South Tyrol (cold European region).

Table 3: Contribution of temperature shocks to the forecast error variance of aggregate GVA, GVA per employee, and investment.

Horizon	Shock	GVA	GVA per employee	Investment
$h = 0$	Winter	0.81	0.61	0.65
	Spring	0.44	0.50	0.76
	Summer	0.41	0.44	0.52
	Fall	0.75	0.47	0.57
$h = 1$	Winter	2.76	1.88	2.93
	Spring	1.41	1.60	2.27
	Summer	1.48	1.99	1.84
	Fall	1.59	0.97	1.70
$h = 2$	Winter	4.87	3.58	5.26
	Spring	2.56	3.34	3.70
	Summer	2.86	3.27	3.16
	Fall	2.91	1.99	3.78
$h = 4$	Winter	7.58	6.64	9.06
	Spring	4.65	6.70	6.72
	Summer	6.05	6.12	6.26
	Fall	4.65	5.97	8.56
$h = 8$	Winter	13.73	12.66	20.03
	Spring	8.08	14.20	13.56
	Summer	11.82	12.27	15.27
	Fall	7.40	14.24	15.05

Notes: Forecast error variance decomposition (FEVD) computed for the level of real aggregate GVA, real aggregate GVA per employee, and gross fixed capital formation (investment) in percent at various horizons. Estimation sample: 1980—2019.

negative effect on poor countries' growth, rich countries are also vulnerable to climate change. To examine whether the level of economic development plays a role in climate risk mitigation, we discriminate the "shock scenario" regime between "rich" and "poor" using either income per capita or an index of regional competitiveness. We, first, group the NUTS2 regions into two sub-groups based on the level of income. In line with Kahn et al. (2021), the regional income is proxied by the GVA at purchasing power parity (PPP) per capita. In particular, a region is defined as a poor region if its average GVA PPP per capita (computed over the 1980 — 2019 period) is below or equal to the median of the empirical distribution, while it is labelled as a rich region if its average (over 1980 — 2019) GVA PPP per capita is above the median of the empirical distribution.[25]

From the upper panel of Figure 7, we can observe that during summer and winter, there is evidence of a marked asymmetric response. In particular, during summer, while rich regions benefit from a modest increase in temperature level (the cumulative effect on GVA is equal to 0.13 % over an eight-year horizon), there is a considerable loss in poor regions equal to −1.84 %. The response of GVA over an eight-year horizon, during winter, is equal to −0.66 % and −2.35 % in rich and poor regions, respectively.

An inspection of the potential transmission channels, i.e., labour productivity (see Figure 7, middle panel) and investment (see Figure 7, lower panel) reveals that the latter plays a more relevant role in explaining the negative impact of temperature shock in poor regions and the resilience observed in rich regions, during winter and summer. More specifically, we find that the effect of rising temperatures on investment is equal to −5.29 % (winter) and −4.87 % (summer) in poor regions, while the response in rich regions is either not statistically different from zero in winter or positive (reaching an increase of 2 % over the last years of the forecast horizon) in summer (see Figure 7, lower panel).

Finally, the empirical exercise is conducted for two different sub-groups of NUTS2 regions that are constructed based on their degree of economic competitiveness, as an alternative to the use of income per capita. As a proxy of regional competitiveness, we use the European Regional Competitiveness Index (RCI) produced by

25 The median of the average (1980 — 2019) GVA PPP per capita is equal to 17,352.5 euro.

Table 4: Contribution of temperature shocks to the forecast error variance of GVA in different economic sectors.

Horizon	Shock	Agriculture	Industry	Construction	Wholesale and others	Fin & business	Non-market
$h = 0$	Winter	0.99	1.09	0.92	0.54	0.73	0.86
	Spring	0.84	0.44	1.06	0.36	0.54	0.62
	Summer	0.83	0.31	0.60	0.15	0.54	0.63
	Fall	0.52	0.39	0.32	1.00	1.09	0.87
$h = 1$	Winter	2.11	2.75	2.31	1.53	1.89	1.24
	Spring	1.77	1.11	1.70	1.50	1.80	1.29
	Summer	0.95	0.90	1.52	0.73	1.03	1.80
	Fall	1.07	1.10	1.71	1.64	2.39	1.85
$h = 2$	Winter	3.28	4.54	3.81	3.69	3.57	2.25
	Spring	2.59	1.78	2.55	2.89	3.25	2.05
	Summer	1.51	1.60	2.80	2.11	1.61	2.53
	Fall	1.87	1.92	2.94	2.73	4.00	2.83
$h = 4$	Winter	5.75	7.00	8.28	5.49	5.67	5.35
	Spring	4.77	3.81	5.95	4.79	5.49	4.18
	Summer	2.74	3.65	7.10	4.17	3.40	4.87
	Fall	3.57	4.07	6.73	4.70	5.87	5.05
$h = 8$	Winter	9.11	12.73	25.36	7.21	11.83	11.97
	Spring	7.46	7.24	13.19	8.51	10.97	7.87
	Summer	6.43	8.82	19.51	7.14	6.28	10.19
	Fall	7.06	11.11	14.87	7.00	10.98	8.58

Notes: Forecast error variance decomposition (FEVD) computed for the level of GVA of six economic sectors, in percent, at various horizons. The economic sectors are: (*i*) agriculture, forestry and fishing (labelled as agriculture), (*ii*) industry (excluding construction) (labelled as industry), (*iii*) construction, (*iv*) wholesale, retail, transport, accommodation and food services, information and communication (labelled as wholesale and others), (*v*) financial & business services (labelled as fin & business), and (*vi*) non-market services (labelled as non-market). Estimation sample: 1980—2019.

the European Commission which provides a synthetic measure of territorial competitiveness at a NUTS2 level. In particular, we use the 2019 version of the index for the 191 EU NUTS2 regions.[26] The RCI 2019 is constructed by aggregating 11 pillars into three groups, that is basic, efficiency, and innovation.[27] In particular, a region is defined as low competitive if its RCI 2019 is below or equal to the median of the empirical distribution, while a region is defined as high competitive if its RCI 2019 is above the median of the empirical distribution.[28]

26 The RCI 2019 is available for 268 NUTS2 regions of 27 EU countries (plus 35 UK NUTS2 regions): Austria, Belgium, Bulgaria, Croatia, Cyprus, Czech Republic, Germany, Denmark, Estonia, Spain, Finland, France, Greece, Hungary, Ireland, Italy, Lithuania, Luxembourg, Latvia, Malta, Netherlands, Poland, Portugal, Romania, Sweden, Slovenia, Slovakia. To construct the final dataset, we match the European Commission (EC) database with the dataset discussed in Section 3.1 (i.e., 191 NUTS2 regions). In the EC dataset, some regions are grouped into the same NUTS code. This is also due to changes in the NUTS codes that occurred in the various NUTS code classifications (the RCI 2019 index is based on the 2016 NUTS code classification). We assign the RCI index reported in the EC database to the NUTS2 regions in the final dataset (i.e., those based on ARDECO) by comparing the exact full name of the region. In particular, for these regions, we proceed as follows. The RCI 2019 index for *Wien & Niederösterreich* (AT00 is the code in the EC database) is assigned to *Niederösterreich* (AT12) and *Wien* (AT13); the RCI 2019 index for *Rég. de Bruxelles-Cap./Brussels Hfst. Gew. & Vlaams-Brabant & Brabant Wallon* (BE00 is the code in the EC database) is assigned to *Prov. Vlaams-Brabant* (BE24) and *Prov. Brabant Wallon* (BE31); the RCI 2019 index for *Praha & Střední čechy* (CZ00 is the code in the EC database) is assigned to *Praha* (CZ01) and *Střední čechy* (CZ02); the RCI 2019 index for *Berlin & Branderburg* (DE00 is the code in the EC database) is assigned to *Berlin* (DE30) and *Branderburg* (DE40); the RCI 2019 index for *Közép-Magyarország* (HU10 is the code in the EC database) is assigned to *Budapest* (HU11) and *Pest* (HU12); the RCI 2019 index for *Flevoland & Noord-Holland* (NL00 is the code in the EC database) is assigned to *Flevoland* (NL23) and *Noord-Holland* (NL32).

27 The 11 pillars taken into account to construct the RCI 2019 are: institutions, macroeconomic stability, infrastructure, health, basic education, higher education and life long learning, labour market efficiency, market size, technological readiness, business sophistication, and innovation. For more details on the construction of the RCI 2019, see Annoni and Dijkstra (2019).

28 The median of the RCI 2019 is equal to 0.09.

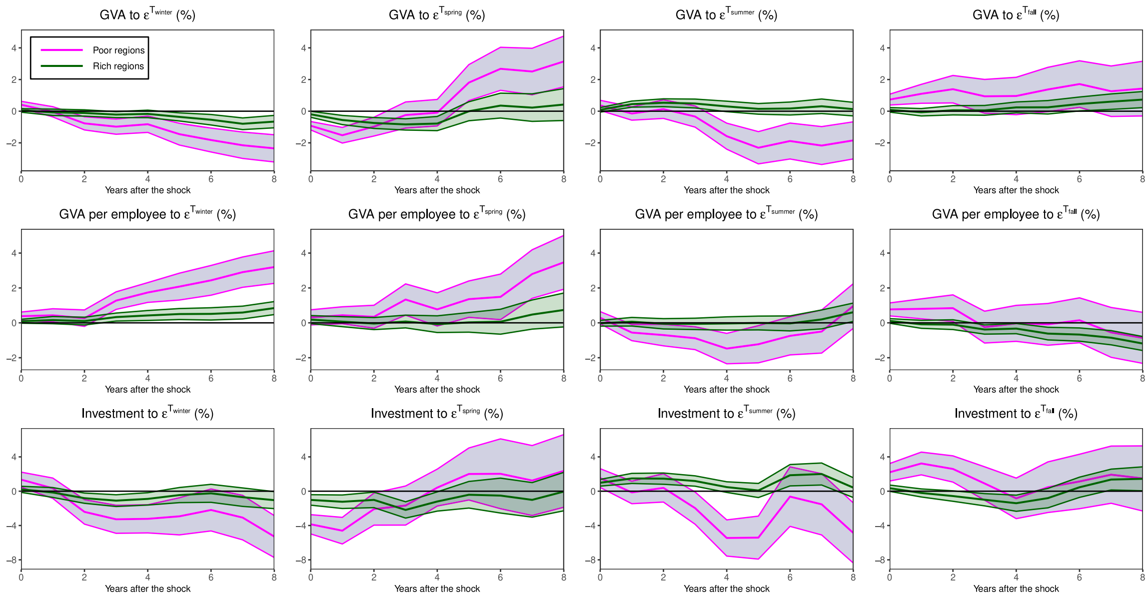

Figure 7: Response of economic activity in rich and poor regions. Notes: Impulse response of the level of real aggregate GVA (upper panel), real aggregate GVA per employee (middle panel), and gross fixed capital formation (investment) (lower panel) to seasonal temperature shocks (in percent), for rich (point estimates reported in green solid line) and poor (point estimates reported in magenta solid line) NUTS2 regions, computed over an eight-year forecast horizon. The charts show the impulse response profile of GVA, GVA per employee, and investment to temperature shocks occurring in winter $\left(\varepsilon^T_{\text{winter}}\right)$, spring $\left(\varepsilon^T_{\text{spring}}\right)$, summer $\left(\varepsilon^T_{\text{summer}}\right)$, and fall $\left(\varepsilon^T_{\text{fall}}\right)$. Each chart displays the impulse response computed for the "shock scenario". A region is labelled as a poor region if its annual GVA at purchasing power parity (PPP) per capita (averaged across 1980 — 2019) is below or equal to the median of the empirical distribution (17,352.5 euro), while a region is labelled as a rich region if its annual GVA PPP per capita (averaged across 1980 — 2019) is above the median of the empirical distribution. For each season, the impulse responses are obtained by setting the shocks ($\tau_{i,s,t}$) as well as the seasonal mean temperature of each region ($\overline{T}_{i,s}$) and the one of each year ($\overline{T}_{s,t}$) at their mean values computed across each subgroup (i.e., poor and rich regions). More specifically, as for poor regions, the conditioning values are set as follows: (*i*) $\tau_{i,s,t} = \text{mean}(\tau_{\text{poor},s,2019})$, i.e., −0.102 (winter), −0.022 (spring), 0.006 (summer), and 0.161 (fall); (*ii*) $\overline{T}_{i,s} = \text{mean}(\overline{T}_{\text{poor},s})$, i.e., 3.7 °C (winter), 13.8 °C (spring), 18.3 °C (summer), and 7.1 °C (fall); (*iii*) $\overline{T}_{s,t} = \text{mean}\left(\overline{T}^{\text{poor}}_{s,2019}\right)$, i.e., 5 °C (winter), 14.6 °C (spring), 19.2 °C (summer), and 8.6 °C (fall). As for rich regions, the conditioning values are set as follows: (*i*) $\tau_{i,s,t} = \text{mean}(\tau_{\text{rich},s,2019})$, i.e., 0.103 (winter), 0.022 (spring), −0.006 (summer), and −0.163 (fall); (*ii*) $\overline{T}_{i,s} = \text{mean}(\overline{T}_{\text{rich},s})$, i.e., 2.2 °C (winter), 12.3 °C (spring), 16.9 °C (summer), and 5.6 °C (fall); (*iii*) $\overline{T}_{s,t} = \text{mean}\left(\overline{T}^{\text{rich}}_{s,2019}\right)$, i.e., 3.7 °C (winter), 13.1 °C (spring), 17.7 °C (summer), and 6.9 °C (fall). The 90 % confidence intervals based on clustered (by region) standard errors are reported for both poor (grey shadow area) and rich (green shadow area) regions. The size of the temperature shocks in each season and both for poor and rich regions is equal to 1 °C increase in the temperature levels. Estimation sample: 1980 — 2019.

The empirical findings in Figure 8 show that highly competitive regions are more resilient than the low competitive ones to temperature shocks. In particular, losses in terms of cumulative GVA growth for low competitive regions during winter and summer are even larger than what we find in Figure 7 (showing results for rich and poor) and they are equal to −2.57 % and −2.54 % over an eight-year horizon, respectively (see Figure 8, upper panel). Furthermore, similarly to the empirical findings for rich and poor regions (see Figure 7), the reduction in GVA observed in summer for low competitive regions is explained by a contraction in both labour productivity and investments, with the latter playing a more relevant role. Moreover, investments drive the negative responses of GVA of low competitive regions in winter (while labour productivity rises due to temperature shocks) (see Figure 8, middle and lower panels).[29]

29 While the empirical findings of a smaller temperature effect on growth in highly competitive regions would suggest that an important role is played by technology (which is one of the pillars underlying the competitiveness indicator) in the resilience to temperature shocks, further investigation should explicitly account for the role played by Total Factor Productivity (TFP). We leave this analysis for future research.

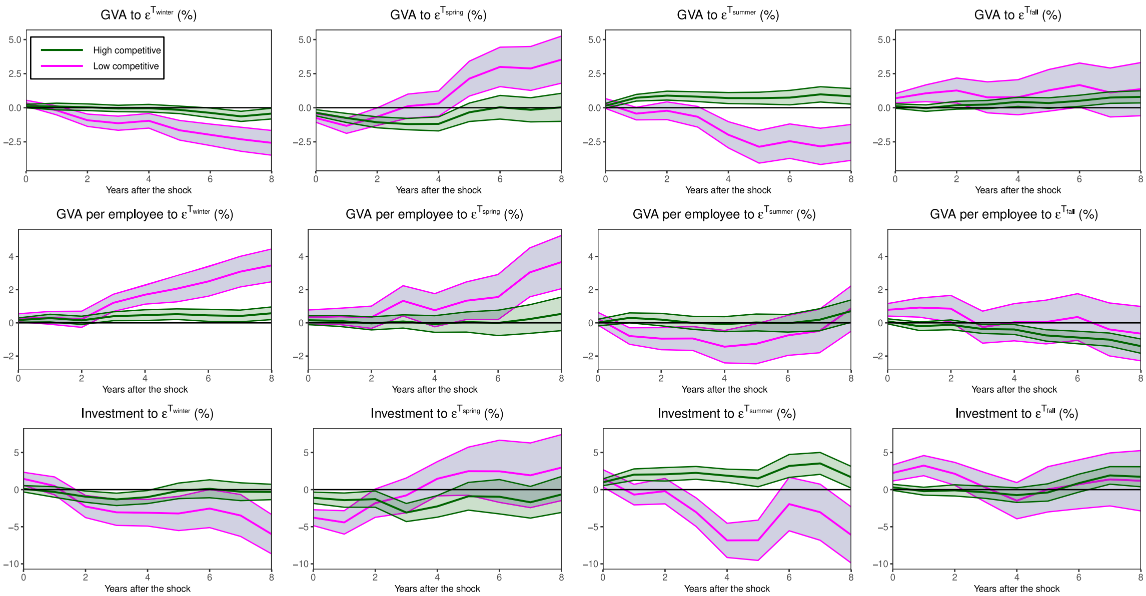

Figure 8: Response of economic activity in high and low competitive regions. Notes: Impulse response of the level of real aggregate GVA (upper panel), real aggregate GVA per employee (middle panel), and gross fixed capital formation (investment) (lower panel) to seasonal temperature shocks (in percent), for high (point estimates reported in green solid line) and low (point estimates reported in magenta solid line) competitive NUTS2 regions, computed over an eight-year forecast horizon. The charts show the impulse response profile of GVA, GVA per employee, and investment to temperature shocks occurring in winter $(\varepsilon^T_{\text{winter}})$, spring $\left(\varepsilon^T_{\text{spring}}\right)$, summer $(\varepsilon^T_{\text{summer}})$, and fall $\left(\varepsilon^T_{\text{fall}}\right)$. Each chart displays the impulse response computed for the "shock scenario". A region is labelled as a low competitive region if its RCI 2019 index is below or equal to the median of the empirical distribution (0.09), while a region is labelled as a high competitive region if its RCI 2019 index is above the median of the empirical distribution. For each season, the impulse responses are obtained by setting the shocks $(\tau_{i,s,t})$ as well as the seasonal mean temperature of each region $(\overline{T}_{i,s})$ and the one of each year $(\overline{T}_{s,t})$ at their mean values computed across each subgroup (i.e., high and low competitive regions). More specifically, as for low competitive regions, the conditioning values are set as follows: (*i*) $\tau_{i,s,t} = \text{mean}(\tau_{\text{low},s,2019})$, i.e., −0.253 (winter), −0.134 (spring), 0.033 (summer), and 0.182 (fall); (*ii*) $\overline{T}_{i,s} = \text{mean}(\overline{T}_{\text{low},s})$, i.e., 3.6 °C (winter), 13.8 °C (spring), 18.6 °C (summer), and 7.1 °C (fall); (*iii*) $\overline{T}_{s,t} = \text{mean}\left(\overline{T}^{\text{low}}_{s,2019}\right)$, i.e., 4.8 °C (winter), 14.5 °C (spring), 19.5 °C (summer), and 8.7 °C (fall). As for high competitive regions, the conditioning values are set as follows: (*i*) $\tau_{i,s,t} = \text{mean}(\tau_{\text{high},s,2019})$, i.e., 0.256 (winter), 0.135 (spring), −0.034 (summer), and −0.184 (fall); (*ii*) $\overline{T}_{i,s} = \text{mean}(\overline{T}_{\text{high},s})$, i.e., 2.2 °C (winter), 12.3 °C (spring), 16.6 °C (summer), and 5.5 °C (fall); (*iii*) $\overline{T}_{s,t} = \text{mean}\left(\overline{T}^{\text{high}}_{s,2019}\right)$, i.e., 3.9 °C (winter), 13.2 °C (spring), 17.4 °C (summer), and 6.8 °C (fall). The 90 % confidence intervals based on clustered (by region) standard errors are reported for both low (grey shadow area) and high (green shadow area) competitive regions. The size of the temperature shocks in each season and both for low and high competitive regions is equal to 1 °C increase in the temperature levels. Estimation sample: 1980 – 2019.

3.5 Projections of Economic Activity

In this section, we perform a counterfactual exercise by computing the projections (over 2020 – 2099) of the cumulative impact of rising temperature, under a scenario of no implementation of climate change mitigation policies, on the GVA of each of the 191 EU NUTS2 regions, as deviations from a baseline assuming that regional temperatures do not increase over the projections period.[30] We compute the regional GVA projections using the estimated coefficients of the non-linear local projection (see equation (2)) fitted to the sample data observed over 1980 – 2019. More specifically, the first regional GVA growth projection, for year 2020, is obtained, first, through the coefficients estimating the impact marginal effect of seasonal temperature shocks on GVA growth using the sample ending in 2019 (corresponding to horizon $h = 0$ in equation (3)). Then, we plug the temperature

30 See the recent studies of Acevedo et al. (2020), Nath et al. (2024), and Bilal and Känzig (2024) on counterfactual analysis producing projections of future temperature effects on output.

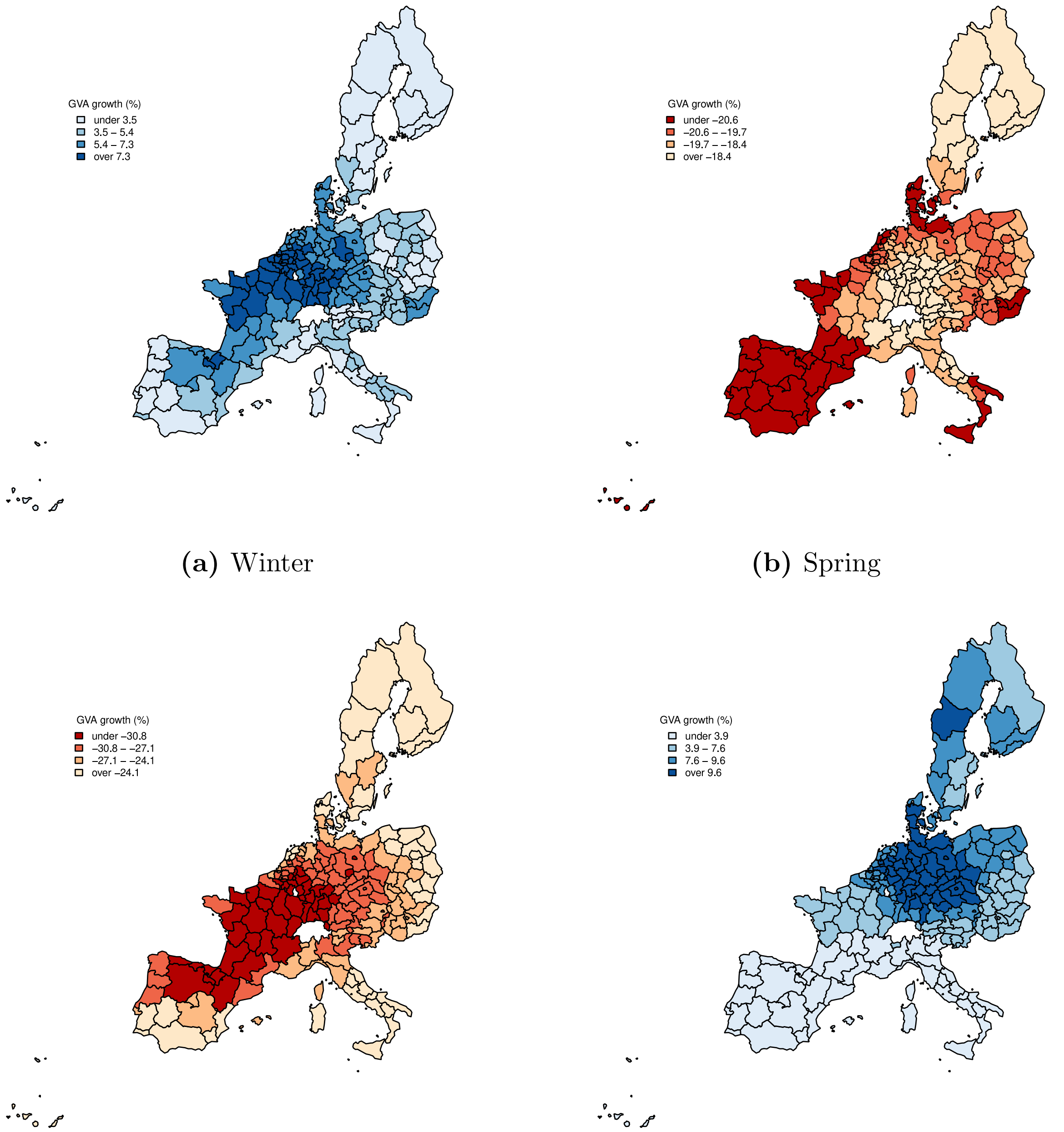

(a) Winter

(b) Spring

(c) Summer

(d) Fall

Figure 9: Projected cumulative impact of global warming on regional GVA in EU. Notes: Projections of the cumulative impact effect of global warming on regional GVA over 2020 — 2099 (deviation from baseline). The seasonal regional forecasts of temperature under the Representative Concentration Pathway (RCP) 8.5 are used to compute the cumulative impact (i.e., at horizon zero) marginal effect of seasonal temperature shocks on GVA growth. The latter is retrieved from the coefficients estimated from the state-dependent local projections (see equation (2)) and by using the temperature projections. For more details, see Section 3.5. *Source for statistical units*: Eurostat, © EuroGeographics for the administrative boundaries.

projections under Representative Concentration Pathway (RCP) 8.5 scenario into equation (3).[31] In particular, we consider: *a*) the projection of the regional seasonal temperature mean (averaged across the sample 1980 − 2020), $\overline{T}_{i,s}$; *b*) the projection of the seasonal global temperature mean in 2020, $\overline{T}_{s,2020}$, obtained as an average of the 2020 temperature projections for each region; *c*) $\tau_{i,s,2020}$ which is the estimated seasonal temperature shock on year 2020 (retrieved from the temperature regression equation, using the projections of seasonal temperatures, over the period 1980 − 2099). Then, we repeat the exercise each following year until 2099, and we compute the cumulative sum returning the projected cumulative impact effect on region-specific GVA growth over the 2020 − 2099 period.[32]

The cumulative sum of the projections under the RCP 8.5 scenario are displayed in Figure 9 and they suggest a high degree of heterogeneity in the regional GVA growth projections across seasons. Overall, the counterfactual exercise shows that winter and fall are the seasons for which projected temperature increases will be beneficial for GVA growth, especially in cold regions. Inspection of Panels A and D of Figure 9 shows that the 191 EU NUTS2 regions will benefit (on average) from rising temperatures in winter (5.23 %) and fall (6.58 %). Inspection of Panels B and C of Figure 9 shows that the average (across the 191 EU regions) cumulative impact of temperature shocks on GVA will be detrimental during spring (−19.59 %) and summer (−27.35 %). The projections of large losses (obtained from the cumulative sum of seasonal temperature effects over the year) are comparable to those of Bilal and Känzig (2024) for the global economy. While the authors emphasize the role of global temperature shock in generating substantial losses, we stress the role played by seasonal temperature effect on growth and their interactions.

4 Conclusions

In this study, we estimate a state-dependent local projection to examine seasonal temperature effects on growth using sub-national data for Europe (the focus is on 191 EU regions). We first contribute to the literature by showing that it is important to account for seasonal temperature shocks and their interactions. The focus on seasonal temperature data is motivated by projections of a temperature rise more concentrated during fall-winter than spring-summer. The impact of each seasonal temperature shock on cumulative growth is non-linear: it is not only conditional on the global seasonal temperature of a given year but also on idiosyncratic factors such as the seasonal shock hitting a given region in a given year. Another methodological contribution is given by the use of a mixed-frequency dataset in a non-linear setting and also by the novelty of modelling state-dependent local projection, which includes non-linear terms in seasonal temperatures (both observed and shocks). The empirical evidence, first, suggests no evidence of adaptation to climate change. Moreover, our empirical findings highlight a heterogeneous degree of vulnerability to seasonal temperature shocks according to the exposure associated with the geographical location and with income per capita (or regional competitiveness) used as proxies of climate risk mitigation factors. A counterfactual exercise, producing GVA projections over 2020 − 2099, shows that EU regions will benefit (loose) from rising temperature in winter-fall (spring-summer).

Our findings have the following policy implications. The empirical model and findings show evidence of a significant contribution from both regional and European-wide temperature effects on GVA growth, supporting current EU initiatives aiming to build climate resilience to be implemented by local policymakers (see, for instance, the EU Mission on Adaptation to Climate Change empowering European regional and local authorities) and through coordination among local authorities (see, for instance, the Global Covenant of Mayors, which is a

31 The RCP 8.5 scenario assumes very high future greenhouse gas emissions and no implementation of climate change mitigation policies. Temperature projections under the RCP 8.5 scenario are the seasonal forecasts of the 2 m air temperature available for the European regions and downloaded from the Copernicus Climate Change Service (2021) database. The projections are based on the regional climate model RegCM4 (ICTP, Italy) and on the global climate model HadGEM2-ES (UK Met Office, UK). Furthermore, the seasonal forecasts of temperature levels for PT30 (*Região Autónoma da Madeira*) are not available, hence we exclude this region from the sample used for the projection exercise.

32 For each year t of the future horizon 2020 − 2099 and for each scenario, the impact marginal effect of seasonal temperature shocks on GVA growth is rescaled by the difference in the global temperature mean occurring between $t - 1$ and t.

global alliance involving cities, local governments, and partners from all sectors of society). Furthermore, the detrimental effect of a temperature increase during winter on agricultural GVA in hot regions suggests an acceleration in policies introducing adapted crops, improved irrigation techniques, field margins and agroforestry, and crop diversification in the southern European regions. Moreover, the detrimental effect on the industry sector (excluding construction) points to policies boosting the green automotive sector. Finally, the evidence of the largest vulnerability to a temperature rise in the construction sector stresses the importance of the EU green buildings pact recently approved aiming to make public and residential buildings more climate-friendly by improving insulation and energy efficiency.

The mixed frequency panel local projection approach could be extended to explore the temperature-growth nexus using monthly (or even higher frequency) observations of temperature, increasing considerably the number of seasonal interaction terms and we leave this for future research.

Appendix A: State-Dependent Local Projections

In this Appendix, we describe the steps followed to derive the state-dependent unrestricted mixed data sampling (U-MIDAS) panel local projection introduced in equation (2). We, first, describe the empirical model specification suggested by Nath et al. (2024) based on a common frequency dataset (yearly data) suggesting the following decomposition of the annual temperature: $T_{i,t} = \overline{T}_i + \overline{T}_t + \tau_{i,t}$, where $\overline{T}_i$ is the annual mean temperature level of each region (computed across years), $\overline{T}_t$ is the annual mean temperature level of each year (computed across regions or countries), and $\tau_{i,t}$ denotes innovations to temperature in each region (or country) and year. The temperature decomposition is, then, replaced by Nath et al. (2024) in a quadratic-in-temperature regression put forward by Burke et al. (2015):

$$\Delta y_{i,t} = \beta T_{i,t} + \Psi T_{i,t}^2 + \delta' X_{i,t} + \mu_i + \mu_t + \varepsilon_{i,t} \tag{7}$$

where $\Delta y_{i,t}$ is the growth rate of the proxy of economic activity observed in region i at year t, $T_{i,t}$ is the annual temperature level, $X_{i,t}$ is a set of control variables (including lagged variables), and μ_i and μ_t are region- and year-fixed effects. The aforementioned substitution allows to model state dependency in the effect of temperature on output growth.

Differently from Nath et al. (2024), which uses annual temperature series, we rely on higher frequency (i.e., seasonal) data on temperature, assuming that the annual temperature ($T_{i,t}$) is computed as the average across four seasons (i.e., winter, spring, summer, and fall), that is $T_{i,t} = 1/4\sum_{s=1}^{4} T_{i,s,t}$, where $T_{i,s,t}$ is the level of temperature observed in region i, at season s, and at year t. Consequently, we focus on the following decomposition of each seasonal temperature series ($T_{i,t}^{(s)}$):

$$T_{i,t}^{(s)} = \overline{T}_i^{(s)} + \overline{T}_t^{(s)} + \tau_{i,t}^{(s)} \tag{8}$$

where $\overline{T}_i^{(s)}$ is the seasonal mean temperature level of region i, $\overline{T}_t^{(s)}$ is the seasonal mean temperature level of each year t, and $\tau_{i,t}^{(s)}$ is the seasonal temperature shock hitting region i at year t. After substituting equations (8) into (7) and ignoring the terms that vary only by region ($\overline{T}_i^{(s)}$) and year ($\overline{T}_t^{(s)}$), that are captured by the region- and year-fixed effects, we can rewrite the specification in equation (7) as follows:

$$\begin{aligned}\Delta y_{i,t} = \frac{1}{4}\beta\sum_{s=1}^{4}\tau_{i,s,t} + \frac{1}{16}\psi\Bigg(&\sum_{s=1}^{4}\tau_{i,s,t}^2 + 2\sum_{\substack{s,r=1\\ s<r}}^{4}\tau_{i,s,t}\tau_{i,r,t} + 2\sum_{s=1}^{4}\sum_{r=1}^{4}\tau_{i,s,t}\overline{T}_{i,r}\\ &+ 2\sum_{s=1}^{4}\sum_{r=1}^{4}\tau_{i,s,t}\overline{T}_{r,t}\Bigg) + \delta' X_{i,t} + \mu_i + \mu_t + \varepsilon_{i,t}\end{aligned} \tag{9}$$

Hence, as described by equation (9), the growth rate of the annual proxy of economic activity ($\Delta y_{i,t}$) can be expressed as a function of non-linear terms involving seasonal temperatures, both observed and shocks, together with the linear term ($\tau_{i,s,t}$) and with the control variables and the region- and year-fixed effects. The set of explanatory variables in equation (9) is, then, used in the panel local projection regression given by equation (2). In line with Nath et al. (2024), to investigate the effect of seasonal temperature shocks on economic activity, we follow a two-step approach. In the first step, we estimate innovations to seasonal temperatures ($\tau_{i,t}^{(s)}$) by regressing the level of temperature observed in each season ($T_{i,t}^{(s)}$) onto its lags and the interactions of the lags with the seasonal mean temperature of each region and the seasonal mean temperature of each year (see equation (1)). In the second step, we use jointly the four time series of residuals obtained from equation (1) to estimate the effects of seasonal temperature shocks ($\tau_{i,s,t}$) on proxies of regional economic activity by using local projections methods, introduced by Jordà (2005), for panel data. Given that the data are sampled at a different frequency (i.e., the level of temperature is available at a seasonal frequency, while the proxy of economic activity is sampled annually), we rely on a MIDAS approach and we estimate the state-dependent U-MIDAS panel local projection described in equation (2).

Appendix B: Panel Regression Estimation

In this Appendix, we discuss the results obtained from the estimation of the U-MIDAS panel local projection (see equation (2)) on impact (i.e., at horizon zero).[33] More specifically, we estimate the following state-dependent U-MIDAS panel regression using seasonal temperature series:

$$y_{i,t} - y_{i,t-1} = \sum_{s=1}^{4} \beta_s \tau_{i,s,t} + \sum_{s=1}^{4} \eta_s \tau_{i,s,t}^2 + \sum_{\substack{s,r=1 \\ s<r}}^{4} \phi_{s,r} \tau_{i,s,t} \tau_{i,r,t} + \sum_{s=1}^{4} \sum_{r=1}^{4} \theta_{s,r} \tau_{i,s,t} \overline{T}_{i,r} + \sum_{s=1}^{4} \sum_{r=1}^{4} \gamma_{s,r} \tau_{i,s,t} \overline{T}_{r,t} + \delta' X_{i,t} + \mu_i + \mu_t + \varepsilon_{i,t|t-1} \tag{10}$$

For more details on the linear and non-linear terms entering equation (10), see Section 2. In Table B.1, we report the estimates for three alternative dependent variables: (*i*) the growth rate of the aggregate real GVA (ΔGVA), (*ii*) the growth rate of the aggregate real GVA per employee (ΔGVA per employee), and (*iii*) the growth rate of gross fixed capital formation (ΔInvestment).[34] As can be seen from Table B.1, there is no evidence of statistically significant effect of seasonal temperature shocks on the proxies of economic growth, i.e., focusing on the linear ($\tau_{i,s,t}$) and quadratic $\left(\tau_{i,s,t}^2\right)$ terms, for $s\ =$ winter, spring, summer, fall. Evidence of statistically significant coefficients shows up mostly for the coefficients associated with the interactions between seasonal temperature shocks and with those between seasonal temperature shocks and observed seasonal temperatures. The empirical evidence in Table B.1 highlights the role played by continent-wide seasonal temperature varying across years where statistical significance shows up not only with the coefficients associated with the region-specific constants ($\overline{T}_{i,r}$) but also with the ones associated with the continent-wide constants ($\overline{T}_{r,t}$). These results support the inclusion of the interaction terms involving seasonal temperature shocks (and observed seasonal temperature) in the proposed state-dependent U-MIDAS panel local projection. Furthermore, we compare the fit of the non-linear mixed-frequency panel regression in equation (10) with the one of a non-linear common-frequency panel regression, involving annual temperature series (i.e., average across seasonal temperatures). In particular, in line with Nath et al. (2024), we estimate the following state-dependent common-frequency panel regression:

33 The results for the remaining forecast horizons are available upon request.

34 In this Appendix, we refer to the first-difference (of the log transformation) of the dependent variable since the long-difference (i.e., the one used in the U-MIDAS panel local projection discussed in Section 2) and the first-difference coincide for horizon zero.

Table B.1: Estimates of the state-dependent mixed-frequency panel regression.

Dependent variable:	**ΔGVA**	**ΔGVA per employee**	**ΔInvestment**
$\tau_{i,\text{winter},t}$	0.039	−0.745	−8.992**
	(1.624)	(1.504)	(4.219)
$\tau_{i,\text{spring},t}$	0.109	−1.111	6.712
	(1.655)	(1.847)	(4.281)
$\tau_{i,\text{summer},t}$	3.518*	−0.701	2.475
	(2.080)	(2.209)	(5.587)
$\tau_{i,\text{fall},t}$	−2.237	−3.525*	−7.472
	(1.972)	(2.073)	(5.547)
$\tau^2_{i,\text{winter},t}$	0.006	0.054	0.144
	(0.048)	(0.049)	(0.125)
$\tau^2_{i,\text{spring},t}$	0.033	−0.126	0.578**
	(0.089)	(0.090)	(0.287)
$\tau^2_{i,\text{summer},t}$	−0.055	−0.049	0.023
	(0.097)	(0.107)	(0.315)
$\tau^2_{i,\text{fall},t}$	0.093	0.058	0.148
	(0.057)	(0.050)	(0.148)
$\tau_{i,\text{winter},t} \times \tau_{i,\text{spring},t}$	−0.025	0.132	−0.499*
	(0.122)	(0.114)	(0.279)
$\tau_{i,\text{winter},t} \times \tau_{i,\text{summer},t}$	0.194**	0.128	0.914***
	(0.097)	(0.097)	(0.218)
$\tau_{i,\text{winter},t} \times \tau_{i,\text{fall},t}$	0.132	0.035	−0.266*
	(0.098)	(0.097)	(0.159)
$\tau_{i,\text{spring},t} \times \tau_{i,\text{summer},t}$	−0.149	0.272	−0.922**
	(0.139)	(0.171)	(0.396)
$\tau_{i,\text{spring},t} \times \tau_{i,\text{fall},t}$	−0.197*	−0.096	−0.478
	(0.102)	(0.098)	(0.292)
$\tau_{i,\text{summer},t} \times \tau_{i,\text{fall},t}$	0.316***	0.095	0.653***
	(0.097)	(0.104)	(0.223)
$\tau_{i,\text{winter},t} \times \overline{T}_{i,\text{winter}}$	0.029	−0.084	0.437***
	(0.075)	(0.069)	(0.159)
$\tau_{i,\text{winter},t} \times \overline{T}_{i,\text{spring}}$	0.126**	0.067	−0.126
	(0.059)	(0.073)	(0.160)
$\tau_{i,\text{winter},t} \times \overline{T}_{i,\text{summer}}$	−0.084	−0.087	0.090
	(0.061)	(0.057)	(0.122)
$\tau_{i,\text{winter},t} \times \overline{T}_{i,\text{fall}}$	−0.021	0.127*	−0.367**
	(0.094)	(0.074)	(0.182)
$\tau_{i,\text{spring},t} \times \overline{T}_{i,\text{winter}}$	−0.038	−0.121	0.338
	(0.167)	(0.152)	(0.460)
$\tau_{i,\text{spring},t} \times \overline{T}_{i,\text{spring}}$	−0.273***	0.178	−0.655**
	(0.098)	(0.117)	(0.276)
$\tau_{i,\text{spring},t} \times \overline{T}_{i,\text{summer}}$	0.285***	−0.049	0.890**
	(0.099)	(0.091)	(0.383)
$\tau_{i,\text{spring},t} \times \overline{T}_{i,\text{fall}}$	0.014	0.004	−0.555
	(0.222)	(0.194)	(0.714)
$\tau_{i,\text{summer},t} \times \overline{T}_{i,\text{winter}}$	0.033	0.125	−0.585
	(0.144)	(0.131)	(0.373)
$\tau_{i,\text{summer},t} \times \overline{T}_{i,\text{spring}}$	−0.132	−0.075	−0.070
	(0.126)	(0.128)	(0.466)
$\tau_{i,\text{summer},t} \times \overline{T}_{i,\text{summer}}$	0.135	0.064	−0.038
	(0.108)	(0.104)	(0.324)
$\tau_{i,\text{summer},t} \times \overline{T}_{i,\text{fall}}$	−0.013	−0.064	0.637
	(0.152)	(0.133)	(0.456)
$\tau_{i,\text{fall},t} \times \overline{T}_{i,\text{winter}}$	0.202*	0.166	0.428*
	(0.112)	(0.109)	(0.238)

Table B.1: (continued)

Dependent variable:	ΔGVA	ΔGVA per employee	ΔInvestment
$\tau_{i,\text{fall},t} \times \overline{T}_{i,\text{spring}}$	−0.071	−0.066	−0.502
	(0.077)	(0.086)	(0.352)
$\tau_{i,\text{fall},t} \times \overline{T}_{i,\text{summer}}$	0.009	0.035	0.223
	(0.060)	(0.060)	(0.213)
$\tau_{i,\text{fall},t} \times \overline{T}_{i,\text{fall}}$	−0.151	−0.146	−0.204
	(0.117)	(0.114)	(0.299)
$\tau_{i,\text{winter},t} \times \overline{T}_{\text{winter},t}$	0.047	−0.072	0.110
	(0.042)	(0.044)	(0.117)
$\tau_{i,winter,t} \times \overline{T}_{spring,t}$	0.153*	0.203**	0.181
	(0.084)	(0.080)	(0.192)
$\tau_{i,\text{winter},t} \times \overline{T}_{\text{summer},t}$	−0.171***	−0.145**	0.373*
	(0.064)	(0.069)	(0.203)
$\tau_{i,\text{winter},t} \times \overline{T}_{\text{fall},t}$	0.118*	0.161**	0.130
	(0.066)	(0.064)	(0.252)
$\tau_{i,\text{spring},t} \times \overline{T}_{\text{winter},t}$	−0.188***	0.226***	−0.655***
	(0.072)	(0.085)	(0.230)
$\tau_{i,\text{spring},t} \times \overline{T}_{\text{spring},t}$	−0.278**	−0.240*	0.182
	(0.122)	(0.133)	(0.258)
$\tau_{i,\text{spring},t} \times \overline{T}_{\text{summer},t}$	0.207**	0.137	−0.326
	(0.090)	(0.105)	(0.219)
$\tau_{i,\text{spring},t} \times \overline{T}_{\text{fall},t}$	−0.158*	0.003	−0.952***
	(0.095)	(0.089)	(0.258)
$\tau_{i,\text{summer},t} \times \overline{T}_{\text{winter},t}$	0.024	−0.014	0.038
	(0.056)	(0.056)	(0.141)
$\tau_{i,\text{summer},t} \times \overline{T}_{\text{spring},t}$	−0.067	−0.003	−0.261
	(0.112)	(0.117)	(0.291)
$\tau_{i,\text{summer},t} \times \overline{T}_{\text{summer},t}$	−0.352***	−0.032	−0.214
	(0.119)	(0.128)	(0.250)
$\tau_{i,\text{summer},t} \times \overline{T}_{\text{fall},t}$	0.435***	0.183*	0.702***
	(0.079)	(0.094)	(0.210)
$\tau_{i,\text{fall},t} \times \overline{T}_{\text{winter},t}$	0.094*	0.028	0.319*
	(0.051)	(0.064)	(0.164)
$\tau_{i,\text{fall},t} \times \overline{T}_{\text{spring},t}$	0.219*	0.154	0.596**
	(0.121)	(0.110)	(0.237)
$\tau_{i,\text{fall},t} \times \overline{T}_{\text{summer},t}$	−0.033	0.059	−0.019
	(0.098)	(0.104)	(0.257)
$\tau_{i,\text{fall},t} \times \overline{T}_{\text{fall},t}$	0.123	0.167**	0.277
	(0.092)	(0.083)	(0.232)
$T_{i,\text{winter},t-1}$	−0.028	0.025	−0.459**
	(0.067)	(0.078)	(0.183)
$T_{i,\text{winter},t-2}$	0.145***	0.125**	−0.159
	(0.052)	(0.052)	(0.144)
$T_{i,\text{spring},t-1}$	−0.165**	−0.177**	0.276
	(0.072)	(0.077)	(0.225)
$T_{i,\text{spring},t-2}$	−0.125	−0.308***	0.233
	(0.084)	(0.078)	(0.237)
$T_{i,\text{summer},t-1}$	0.189**	0.078	0.645**
	(0.080)	(0.092)	(0.266)
$T_{i,\text{summer},t-2}$	0.065	−0.054	0.199
	(0.063)	(0.071)	(0.235)
$T_{i,\text{fall},t-1}$	−0.240***	−0.215***	−0.346*
	(0.069)	(0.073)	(0.201)
$T_{i,\text{fall},t-2}$	0.016	−0.065	−0.403**
	(0.054)	(0.056)	(0.162)

Table B.1: (continued)

Dependent variable:	ΔGVA	ΔGVA per employee	ΔInvestment
$P_{i,\text{winter},t-1}$	−0.665	0.354	−1.416
	(0.485)	(0.562)	(1.418)
$P_{i,\text{winter},t-2}$	−0.535	1.338**	−6.324***
	(0.549)	(0.565)	(1.860)
$P_{i,\text{spring},t-1}$	−1.378**	0.205	−0.251
	(0.646)	(0.668)	(2.037)
$P_{i,\text{spring},t-2}$	−2.187***	−1.413*	−8.182***
	(0.807)	(0.781)	(2.360)
$P_{i,\text{summer},t-1}$	0.806	−0.505	7.635***
	(0.654)	(0.716)	(2.033)
$P_{i,\text{summer},t-2}$	−1.514	−1.439	−4.805*
	(1.026)	(0.979)	(2.621)
$P_{i,\text{fall},t-1}$	1.842***	0.358	3.543**
	(0.643)	(0.917)	(1.766)
$P_{i,\text{fall},t-2}$	−0.031	−0.872	0.254
	(0.586)	(0.620)	(1.993)
$\Delta\text{GVA}_{i,t-1}$	−0.018		
	(0.033)		
$\Delta\text{GVA}_{i,t-2}$	0.040		
	(0.031)		
$\Delta\text{GVA per employee}_{i,t-1}$		−0.055*	
		(0.031)	
$\Delta\text{GVA per employee}_{i,t-2}$		−0.016	
		(0.026)	
$\Delta\text{Investment}_{i,t-1}$			−0.096***
			(0.031)
$\Delta\text{Investment}_{i,t-2}$			−0.076
			(0.063)
Observations	6,563	6,461	6,567
R^2	0.3428	0.2338	0.2576

Notes: Estimates (in percent) of the U-MIDAS panel regression described in equation (10) (see also equation (2)) for alternative dependent variables: growth rate of real aggregate GVA (ΔGVA), growth rate of real aggregate GVA per employee (ΔGVA per employee), and growth rate of gross fixed capital formation (ΔInvestment). Each specification includes both region- and year-fixed effects. Standard errors clustered by region are reported in brackets. Estimation sample: 1980–2019. ***p-value < 0.01, **p-value < 0.05, *p-value < 0.1.

$$y_{i,t} - y_{i,t-1} = \tilde{\beta}\tau_{i,t} + \tilde{\eta}\tau_{i,t}^2 + \tilde{\theta}\tau_{i,t}\overline{T}_i + \tilde{\gamma}\tau_{i,t}\overline{T}_t + \tilde{\delta}' Z_{i,t} + \mu_i + \mu_t + \xi_{i,t|t-1} \tag{11}$$

where $y_{i,t}$ is the log transformation of the proxy of economic activity, $\overline{T}_i$ is the region's historical annual temperature, $\overline{T}_t$ is the annual mean temperature computed across regions, and $\tau_{i,t}$ is the annual temperature shock.[35] Moreover, $Z_{i,t}$ is the vector of control variables, including two lags of annual temperature ($T_{i,t}$), two lags of annual precipitation ($P_{i,t}$), and two lags of the dependent variable. Finally, μ_i and μ_t are the region- and year-fixed effects. We test for the following multiple linear restrictions:

$$\frac{1}{4}\beta_1 = \frac{1}{4}\beta_2 = \frac{1}{4}\beta_3 = \frac{1}{4}\beta_4$$
$$\frac{1}{4}\eta_1 = \frac{1}{4}\eta_2 = \frac{1}{4}\eta_3 = \frac{1}{4}\eta_4$$

35 Shocks to annual temperature ($\tau_{i,t}$) are estimated by using the same approach discussed in Section 2 for seasonal temperature shocks. More specifically, the annual temperature shock is the residual of the following panel regression fitted to annual temperature series: $T_{i,t} = \sum_{j=1}^{p}\rho_j T_{i,t-j} + \sum_{j=1}^{p}\lambda_j T_{i,t-j}\overline{T}_i + \sum_{j=1}^{p}\omega_j T_{i,t-j}\overline{T}_t + \alpha_i + \alpha_t + \tau_{i,t}$, where p is set equal to two.

$$\phi_{12} = \phi_{13} = \phi_{14} = \phi_{23} = \phi_{24} = \phi_{34} = 0$$
$$\frac{1}{16}\theta_{11} = \frac{1}{16}\theta_{12} = \ldots = \frac{1}{16}\theta_{14} = \ldots \frac{1}{16}\theta_{24} = \ldots = \frac{1}{16}\theta_{44}$$
$$\frac{1}{16}\gamma_{11} = \frac{1}{16}\gamma_{12} = \ldots = \frac{1}{16}\gamma_{14} = \ldots \frac{1}{16}\gamma_{24} = \ldots = \frac{1}{16}\gamma_{44} \tag{12}$$

This returns a set of forty-two restrictions. After including also those related to the control variables (i.e., an extra set of twelve restrictions), we test for a total of fifty-four restrictions. We use an F statistics to test the null hypothesis given by equation (12) and, for this purpose, we estimate the residual sum squares associated with the (restricted) non-linear common-frequency model described in equation (11) and the one for the (unrestricted) non-linear mixed-frequency model (see equation (10)). The F test rejects the null hypothesis supporting the use of the unrestricted model in equation (10).[36]

References

Acevedo, Sebastian, Mico Mrkaic, Natalija Novta, Evgenia Pugacheva, and Petia Topalova. 2020. “The Effects of Weather Shocks on Economic Activity: What are the Channels of Impact?” *Journal of Macroeconomics* 65: 103207.

Alessandri, Piergiorgio, and Haroon Mumtaz. 2025. “The Macroeconomic Cost of Temperature Risk.” *Journal of International Economics* 158: 104157.

Annoni, Paola, and Lewis Dijkstra. 2019. “The EU Regional Competitiveness Index 2019.” *European Commission Working Papers*. https://ec.europa.eu/regional_policy/information-sources/publications/working-papers/2019/the-european-regional-competitiveness-index-2019_en (accessed October 21, 2024).

Ballester, Joan, Marcos Quijal-Zamorano, Raúl Fernando Méndez Turrubiates, Ferran Pegenaute, François R. Herrmann, Jean Marie Robine, et al. 2023. “Heat-Related Mortality in Europe During the Summer of 2022.” *Nature Medicine* 29: 1857−66.

Bilal, Adrien, and Diego R. Känzig. 2024. “The Macroeconomic Impact of Climate Change: Global vs. Local Temperature.” *NBER Working Paper No. 32450*. National Bureau of Economic Research.

Burke, Marshall, W. Matthew Alampay Davis, and Noah S. Diffenbaugh. 2018. “Large Potential Reduction in Economic Damages Under UN Mitigation Targets.” *Nature* 557: 549−53.

Burke, Marshall, Solomon M. Hsiang, and Miguel Edward. 2015. “Global Non-Linear Effect of Temperature on Economic Production.” *Nature* 527: 235−9.

Ciccarelli, Matteo, Friderike Kuik, and Catalina Martínez Hernández. 2024. “The Asymmetric Effects of Temperature Shocks on Inflation in the Largest Euro Area Countries.” *European Economic Review* 168: 104805.

Colacito, Riccardo, Bridget Hoffmann, and Toan Phan. 2019. “Temperature and Growth: A Panel Analysis of the United States.” *Journal of Money, Credit, and Banking* 51 (2-3): 313−68.

Copernicus Climate Change Service. 2020. “Climate and Energy Indicators for Europe from 1979 to Present Derived from Reanalysis.” Copernicus Climate Change Service (C3S) Climate Data Store (CDS). https://cds.climate.copernicus.eu/datasets/sis-energy-derived-reanalysis?tab=overview (accessed June 6, 2022).

Copernicus Climate Change Service. 2021. “Climate and Energy Indicators for Europe from 2005 to 2100 Derived from Climate Projections.” Copernicus Climate Change Service (C3S) Climate Data Store (CDS). https://cds.climate.copernicus.eu/datasets/sis-energy-derived-projections?tab=overview (accessed October 2, 2024).

Copernicus Climate Change Service/ECMWF. 2022. “Global Climate Highlights 2022 [Online].” *The 2022 Annual Climate Summary*. https://climate.copernicus.eu/global-climate-highlights-2022 (accessed June 13, 2023).

De Bandt, Olivier, Luc Jacolin, and Lemaire Thibault. 2021. “Climate Change in Developing Countries: Global Warming Effects, Transmission Channels and Adaptation Policies.” *Banque de France Working Paper No. 822*. https://publications.banque-france.fr/en/climate-change-developing-countries-global-warming-effects-transmission-channels-and-adaptation (accessed March 25, 2024).

Dell, Melissa, Benjamin F. Jones, and Benjamin A. Olken. 2012. “Temperature Shocks and Economic Growth: Evidence from the Last Half Century.” *American Economic Journal: Macroeconomics* 4 (3): 66−95.

Deryugina, Tatyana, and Solomon M. Hsiang. 2014. “Does the Environment Still Matter? Daily Temperature and Income in the United States.” *NBER Working Paper No. 20750*. National Bureau of Economic Research.

36 We compute the F-statistic for testing the restrictions in equation (12) by using alternative dependent variables (the F-statistic is reported in bracket): ΔGVA (4.05), ΔGVA per employee (3.19), and ΔInvestment (4.25). Results for sectoral GVA are available upon request.

Donadelli, Michael, Marcus Jüppner, Antonio Paradiso, and Christian Schlag. 2021. "Computing Macro-Effects and Welfare Costs of Temperature Volatility: A Structural Approach." *Computational Economics* 58: 347–94.

Donadelli, Michael, Marcus Jüppner, Max Riedel, and Christian Schlag. 2017. "Temperature Shocks and Welfare Costs." *Journal of Economic Dynamics and Control* 82: 331–55.

Donadelli, Michael, Marcus Jüppner, and Sergio Vergalli. 2022. "Temperature Variability and the Macroeconomy: A World Tour." *Environmental and Resource Economics* 83: 221–59.

Du, Ding, Xiaobing Zhao, and Ruihong Huang. 2017. "The Impact of Climate Change on Developed Economies." *Economics Letters* 153: 43–6.

Falk, Martin, and Xiang Lin. 2018. "Sensitivity of Winter Tourism to Temperature Increases over the Last Decades." *Economic Modelling* 71: 174–83.

Fankhauser, Samuel, and Richard S. J. Tol. 2005. "On Climate Change and Economic Growth." *Resource and Energy Economics* 27 (1): 1–17.

Foroni, Claudia, Massimiliano Marcellino, and Christian Schumacher. 2015. "Unrestricted Mixed Data Sampling (MIDAS): MIDAS Regressions with Unrestricted Lag Polynomials." *Journal of the Royal Statistical Society Series A: Statistics in Society* 178 (1): 57–82.

Ghysels, Eric, Arthur Sinko, and Rossen Valkanov. 2007. "MIDAS Regressions: Further Results and New Directions." *Econometric Reviews* 26 (1): 53–90.

Gibney, Garreth, Thomas K. J. McDermott, and John Cullinan. 2023. "Temperature, Morbidity, and Behavior in Milder Climates." *Economic Modelling* 118: 106106.

Gorodnichenko, Yuriy, and Byoungchan Lee. 2020. "Forecast Error Variance Decompositions with Local Projections." *Journal of Business & Economic Statistics* 38 (4): 921–33.

Greßer, Christina, Daniel Meierrieks, and David Stadelmann. 2021. "The Link Between Regional Temperature and Regional Incomes: Econometric Evidence with Sub-National Data." *Economic Policy* 36 (107): 523–50.

Groom, Ben, Manuel Linsenmeier, and Sefi Roth. 2023. "Some Like it Cold: Heterogeneity in the Temperature-Economy Relationships of Europe." Mimeo. https://osf.io/preprints/socarxiv/tcnad_v1 (accessed November 1, 2023).

Jordà, Òscar. 2005. "Estimation and Inference of Impulse Responses by Local Projections." *American Economic Review* 95 (1): 161–82.

Kahn, Matthew E., Kamiar Mohaddes, Ryan N. C. Ng, M. Hashem Pesaran, Mehdi Raissi, and Jui-Chung Yang. 2021. "Long-Term Macroeconomic Effects of Climate Change: A Cross-Country Analysis." *Energy Economics* 104: 105624.

Kalkuhl, Matthias, and Leonie Wenz. 2020. "The Impact of Climate Conditions on Economic Production. Evidence from a Global Panel of Regions." *Journal of Environmental Economics and Management* 103: 102360.

Kolstad, Charles D., and Frances C. Moore. 2020. "Estimating the Economic Impacts of Climate Change Using Weather Observations." *Review of Environmental Economics and Policy* 14 (1). https://doi.org/10.1093/reep/rez024.

Kotz, Maximilian, Leonie Wenz, Annika Stechemesser, Matthias Kalkuhl, and Anders Levermann. 2021. "Day-to-Day Temperature Variability Reduces Economic Growth." *Nature Climate Change* 11: 319–25.

Li, Ning, Kou Bai, Zhengtao Zhang, Jieling Feng, Xi Chen, and Li Liu. 2019. "The Nonlinear Relationship Between Temperature Changes and Economic Development for Individual Provinces in China." *Theoretical and Applied Climatology* 137: 2477–86.

Linsenmeier, Manuel. 2023. "Temperature Variability and Long-Run Economic Development." *Journal of Environmental Economics and Management* 121: 102840.

Linsenmeier, Manuel. 2024. "Seasonal Temperature Variability and Economic Cycles." *Journal of Macroeconomics* 79: 103568.

Mohaddes, Kamiar, Ryan N. C. Ng, M. Hashem Pesaran, Mehdi Raissi, and Jui-Chung Yang. 2023. "Climate Change and Economic Activity: Evidence from US States." *Oxford Open Economics* 2: odac010.

Nath, Ishan B., Valerie A. Ramey, and Peter J. Klenow. 2024. "How Much Will Global Warming Cool Global Growth?" *NBER Working Paper No. 32761*. National Bureau of Economic Research.

Newell, Richard G., Brian C. Prest, and Steven E. Sexton. 2021. "The GDP-Temperature Relationship: Implications for Climate Change Damages." *Journal of Environmental Economics and Management* 108: 102445.

Nguyen, Ha Minh. 2024. "Beyond the Annual Averages: Impact of Seasonal Temperature on Employment Growth in US Counties." *Journal of Environmental Economics and Management* 125: 102946.

Olper, Alessandro, Maurizio Maugeri, Veronica Manara, and Valentina Raimondi. 2021. "Weather, Climate and Economic Outcomes: Evidence from Italy." *Ecological Economics* 189: 107156.

Zhao, Xiaobing, Mason Gerety, and Nicolai V. Kuminoff. 2018. "Revisiting the Temperature-Economic Growth Relationship Using Global Subnational Data." *Journal of Environmental Management* 223: 537–44.

Supplementary Material: This article contains supplementary material (https://doi.org/10.1515/snde-2025-0108).